THE EFFECT OF FLAP TO AERODYNAMICS PERFORMANCE OF AIRFOIL

MUHAMMAD DZULZHAFRAIN ILMAN BIN ZULKEFLI

UNIVERSITI TEKNIKAL MALAYSIA MELAKA

THE EFFECT OF FLAP TO AERODYNAMICS PERFORMANCE OF AIRFOIL

MUHAMMAD DZULZHAFRAIN ILMAN BIN ZULKEFLI

This dissertation is submitted to Faculty of Mechanical Engineering in partial fulfilment of the requirements for the degree of Bachelor of Mechanical Engineering (Thermal & Fluids)

Faculty of Mechanical Engineering

UNIVERSITI TEKNIKAL MALAYSIA MELAKA

May 2017

DECLARATION

"I admitted that this report is truly mine except the summaries and extractions where both I clearly knew its sources."

Signature :…………………………………………..

Writer :…………………………………………..

Date :…………………………………………..

APPROVAL

"I admitted that I have read this work and from my opinion it is adequately based on the scopes and quality for the degree of Bachelor of Mechanical Engineering"

(Thermal & Fluids)

Signature :..

Supervisor Name :..

Date :..

DEDICATION

I dedicated this Final Year Project to my lovely parent, Mr Zulkefli Bin Hj Yaacob, Mdm Sulyati Binti Abd Kadir and my family because they always keep supporting me and giving me courage in completing this project. Thankful and appreciation I give to Dr. Nazri Bin Md Daud as my supervisor that always guide me in completing this project. Much appreciation I give to my friends that helps me and guide me in completing this project.

ABSTRACT

Airfoil shapes are designed to provide high lift values at low drag for given flight conditions. Lift is the force generated perpendicular to the direction of travel for an object moving through a fluid (gas or liquid) such as an airfoil in a wind tunnel while drag is the force generated parallel and in opposition to the direction of travel for an object moving through a fluid. Conventional aircraft wings often use moving surfaces (flaps and slats) to adapt to different conditions however this study will just focus on the flap of an airfoil. A NACA 0015 symmetrical airfoil was analyzed to determine the lift and drag coefficient. A 3D airfoil was placed in a test section of a low speed wind tunnel to measure the drag force and lift force. The wind tunnel was operated at a nominal 9.5 m/s. The airfoil, with 130 mm chord and 130 mm span, was analyzed at 0, 5, 10 and 15 degree angles of attack. Besides, this experiment was conducted to compare the result between an airfoil with zero angle of flap and airfoil with angle of flap. Angle of flap has been set at two angle which were 30 and 60 degree angle of flap. Two set of airfoils has been printed for this study. The result shows that airfoil have the highest value coefficient of lift at 60 degree of flap which is 0.664. In addition, throughout the previous research and theoretically, an airplane need a higher value of lift coefficient because once the aircraft is on the ground, the flaps may decrease the effectiveness of the brakes, thus increasing stopping distance, particularly in wet or icy conditions.

ABSTRAK

Bentuk sayap pesawat direka untuk menyediakan nilai angkat tinggi pada heret rendah untuk keadaan penerbangan yang diberikan. Angkat adalah daya yang dihasilkan berserenjang dengan arah perjalanan bagi sesuatu objek bergerak melalui cecair (gas atau cecair) seperti lelayang di dalam terowong angin semasa heret adalah daya dijana selari dan bertentangan dengan arah perjalanan untuk objek bergerak melalui bendalir. Sayap pesawat konvensional sering menggunakan permukaan bergerak (kepak dan selat) untuk menyesuaikan diri dengan keadaan yang berbeza bagaimanapun kajian ini hanya akan memberi tumpuan kepada penutup sayap pesawat. Sayap pewasat NACA 0015 simetri dianalisis untuk menentukan angkat dan heret pekali. Sayap pesawat 3D telah diletakkan di dalam ruang ujian terowong angin kelajuan rendah untuk mengukur daya seret dan angkat berkuat kuasa. Terowong angin telah beroperasi pada nominal 9.5 m / s. Sayap pesawat dengan 130 mm kord dan 130 mm span, dianalisis pada 0, 5, 10 dan 15 darjah sudut serangan. Selain itu, eksperimen ini dijalankan untuk membandingkan keputusan di antara sayap pesawat dengan sudut sifar kepak dan sayap pesawat dengan sudut kepak. Sudut penutup telah ditetapkan pada dua sudut antara 30 dan 60 darjah sudut kepak. Dua sayap pesawat yang telah dicetak untuk kajian ini. Hasilnya menunjukkan bahawa sayap pesawat mempunyai nilai pekali lif tertinggi di 60 darjah kepak yang 0.664. Di samping itu, mengikut kajian sebelumnya dan secara teori, kapal terbang perlu nilai pekali lif yang lebih tinggi kerana apabila pesawat itu berada di atas tanah, kepak boleh mengurangkan keberkesanan brek, sekali gus meningkatkan jarak berhenti, terutamanya dalam keadaan basah atau berais.

ACKNOWLEDGEMENT

Praise to Allah for allowing me to complete my thesis successfully and for giving me good health and mind.

I would like to express my great sincere gratitude to my supervisor Dr Nazri bin Md Daud whose help, suggestions, never ending patience, and valuable and kind guidance brought me up to this achievement. During my thesis study, he spent lots of time on reading my drafts and gave many comments. It is not possible for me complete this study without his help.

A special thanks to Mr Faizal bin Jaafar and Mr Rashdan, with their help I could visit the laboratory of wind tunnel and I learnt a lot of knowledge about wind tunnels there. Special thanks also to my friends who helps and guides me throughout the process.

I would also to extend my appreciation for whom that keeps supporting and encouraging me during hardships. Last but not least, I would like to express my deepest gratitude towards people who help me in completing this thesis indirectly. Especially my family who helps me financially, encouraged morally and mentally.

TABLE OF CONTENT

LIST OF FIGURES

LIST OF TABLES

LIST OF ABBEREVATIONS

NACA	National Advisory Committee for Aeronautics
CFD	Computational Fluid Dynamics
AoA	Angle of Attack
RANS	Reynolds Average Navier–Stokes
MATLAB	Matrix Laboratory
MPH	Miles per Hour
ABS	Acrylonitrile-Butadiene-Styrene
RPM	Revolutions per minute
UV	Ultraviolet
VRI	Vacuum Resin Infusionor

LIST OF SYMBOLS

α	Angle of Attack
Re	Reynolds Number
Ma	Mach Number
Fr	Froude Number
ε/l	Relative Roughness of the Surface
V	Velocity
C_L	Coefficient of Lift
C_D	Coefficient of Drag
ρ	Density
A_S	Surface Area
l	Span (Airfoil Width)
c	Chord (Airfoil Length)
z	Height
γ	Specific Weight
τ	Surface Shear Stress

CHAPTER 1

INTRODUCTION

1.1 BACKGROUND

Wind turbines use wind energy to transform into electrical energy but wind turbines efficiency is not good. Because of that, a number of scientists are investigated over wind turbines and wind turbines parameters. One of the most important parameter of wind turbines is wing because wind hits to the wings and energy of wind is transformed into the mechanical energy by wings. In the literature, wings profiles are called as airfoils. Airfoil profile is the important parameter for wing design because wing efficiency increases depending on airfoil profile, so there are a lot of studies over the airfoil profile as numerical and experimental in the literature.

A fluid flowing past a body, in this case an airfoil has a force exerted on it. Lift is defined to be the component of this force that is perpendicular to the oncoming flow direction. The drag force is the opposite of lift, which is defined to be the component of the fluid-dynamic force parallel to the flow direction. We will explore how the angle of attack changes the amount of lift the airfoil experiences. The angle of attack (α) is the angle between flow and the chord line. The chord line is a straight line between the most forward point and most aft point of the body. We will also study the effects of velocity on lift, if the angle of attack is kept constant and velocity increased we would expect an increase in lift. We will measure the airfoil lift as a function of velocity.

The drag coefficient (C_D) and lift coefficient (C_L) are functions of dimensionless parameters such as Reynolds number (Re), Mach number (Ma), Froude number (Fr) and relative roughness of the surface (ε/l). The lift and drag coefficients are mostly dependent on the shape of the airfoil, NACA 0015 (Figure 1) is a symmetrical airfoil. The shapes play a huge role on the amount of lift and drag generated and will be seen in this experiment. In order to be able to use equations (1), (2) and (3) the velocity needs to be known.

<u>NOTATION</u>

V : Velocity

C_L : Coefficient of Lift

C_D : Coefficient of Drag

ρ : Density

A_S : Surface Area

l : Span (Airfoil Width)

c : Chord (Airfoil Length)

z : Height

γ : Specific Weight

The lift is a function of dynamic pressure, surface area and lift coefficient as shown in Equation (1).

$$L = \frac{1}{2}\rho V^2 A_S C_L \tag{1}$$

The drag is a function of dynamic pressure, surface area and drag coefficient as shown in Equation (2).

$$D = \frac{1}{2}\rho V^2 A_S C_D \tag{2}$$

Dynamic Pressure is shown in Equation (3).

$$P_d = \frac{1}{2}\rho V^2 \tag{3}$$

Surface Area (As) is a function of the chord and span and is shown in Equation (4).

$$A_S = cl \tag{4}$$

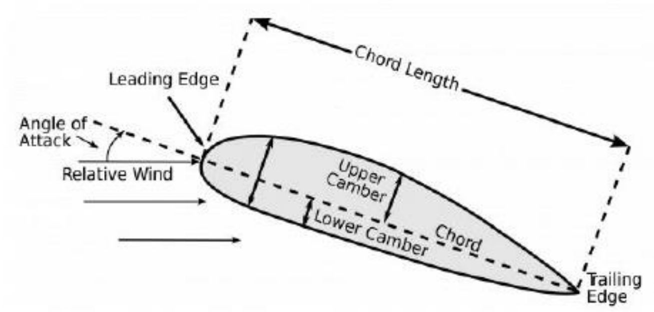

Figure 1 : NACA 0015 Nomenclature

1.2 PROBLEM STATEMENT

Since thin airfoil theory is applicable only to incompressible potential flow, then other means must be used to arrive at the mathematical expression which provide the variation of the airfoil's sectional drag as a function of flap deflection angle. In order to increase the wind capture ability of the wind turbine, many research studies on the lift enhancement method of the wind turbine airfoil have been conducted by scholars at home and abroad. An airfoil with tailing edge flaps has a much higher lift-to-drag ratio than an airfoil without trailing edge flaps.

Among all the lift enhancement methods of trailing edge flaps, the structure of the wind turbine airfoil with discrete trailing edge flaps is simple, the cost of production is low, and it can easily achieve variable angle control. But the aerodynamic performance of the wind turbine airfoil with traditional discrete trailing edge flaps has not been comprehensively studied, and gaps between the flaps and the airfoil main body has an influence on the aerodynamic performance of the airfoil. So it is necessary to optimize the gap structure and study the aerodynamic performance of the discrete trailing edge flaps with different deflection angles. Taking a wind turbine NACA 0015 airfoil as the research object, the structure of the discrete trailing edge flaps was designed, the chord length was set as 130 mm, and the gap between the flap and the main body of airfoil was optimized to make the width of gap an even 1 mm. Then the trailing edge flaps model was established. The flap rotates around the rotate center to form a different flap model at different deflect angles, the deflect angles of the flap varied from 0° - 10°, while the value of angle of attack are at 10° and 20°.

1.3 OBJECTIVE

The objectives of the research are stated below:-

1) To measure the value of drag and lift for NACA 0015 airfoil.
2) To compare both value of drag and lift for base case and actual case.
3) Understand how the angle of attack of an airfoil changes the amount of lift (L vs. α).

1.4 SCOPE OF PROJECT

To fulfill the experimental work, some preparation need to be made:

- A NACA 0015 airfoil with a chord length of 130 mm and span of 130 mm was tested.
- Use fixed value of air velocity.
- To measure C_L and C_D based on a different value angle of attack.
- Study the effect of angle of flap on an airfoil.

1.5 GENERAL METHODOLOGY

The methodology implemented in this research takes the following steps of works:

1.5.1 Fabrication of airfoil

By using a SolidWork software, a NACA 0015 airfoil will be designed referring to its own dimensions with a chord length of 130 mm and span of 130 mm. This experiment was conducted to study the effect of flap to aerodynamics performance of airfoil so that there is a different in drawing this airfoil compared to other design. At the trailing edge of this airfoil, flap is drawn and its length is 20mm from the edge. This helps to change the angle of flap by moving it vertically. The drawing then will be used to perform a 3D printing at a laboratory in faculty of mechanical engineering.

1.5.2 Experimental work

A subsonic wind tunnel was used to determine the lift and drag for the two airfoils at varying angles of attack. The wind tunnel consists of three sections which are nozzle, test section, and exit as shown in Figure 2. Air enters a contraction cone of the nozzle, which is screened by a honeycomb filter to decrease turbulence of the air entering the test section. This contraction cone is followed by the straight test section with the dimensions of 130mm x 130mm (chord x span) in which the airfoil was mounted. The exit consists of an air outflow and a motor-driven fan whose speed is controlled by a frequency drive. A Monarch optical tachometer provides real-time measurements of the fan rotor speed. When the airfoil is already placed, the wind tunnel will run based on a fixed value of air velocity. Angle of attack can be set manually and we only use 2 angle in this experiment. Then the value of lift and drag force are collected to determine the value of C_L and C_D.

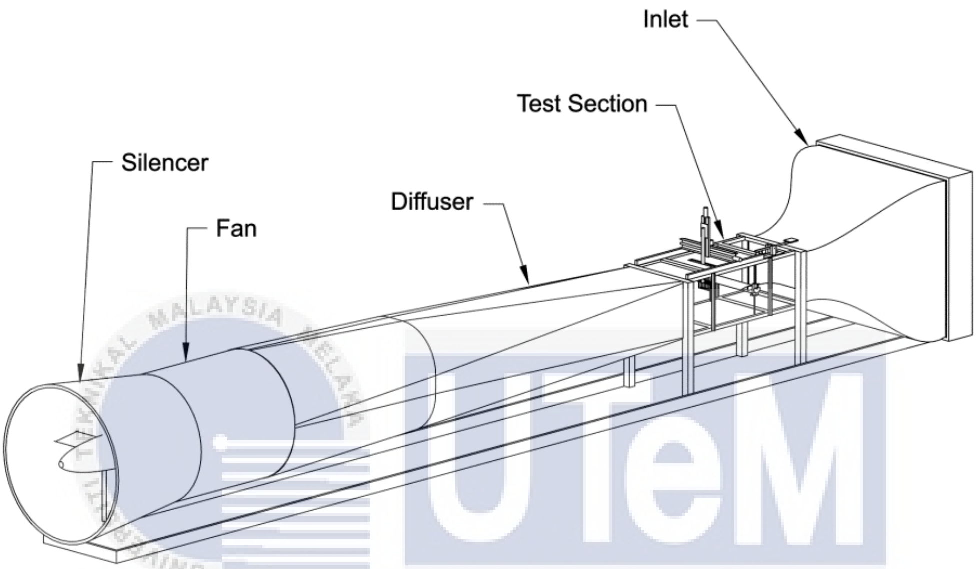

Figure 2 : Wind Tunnel

1.5.3 Flow chart

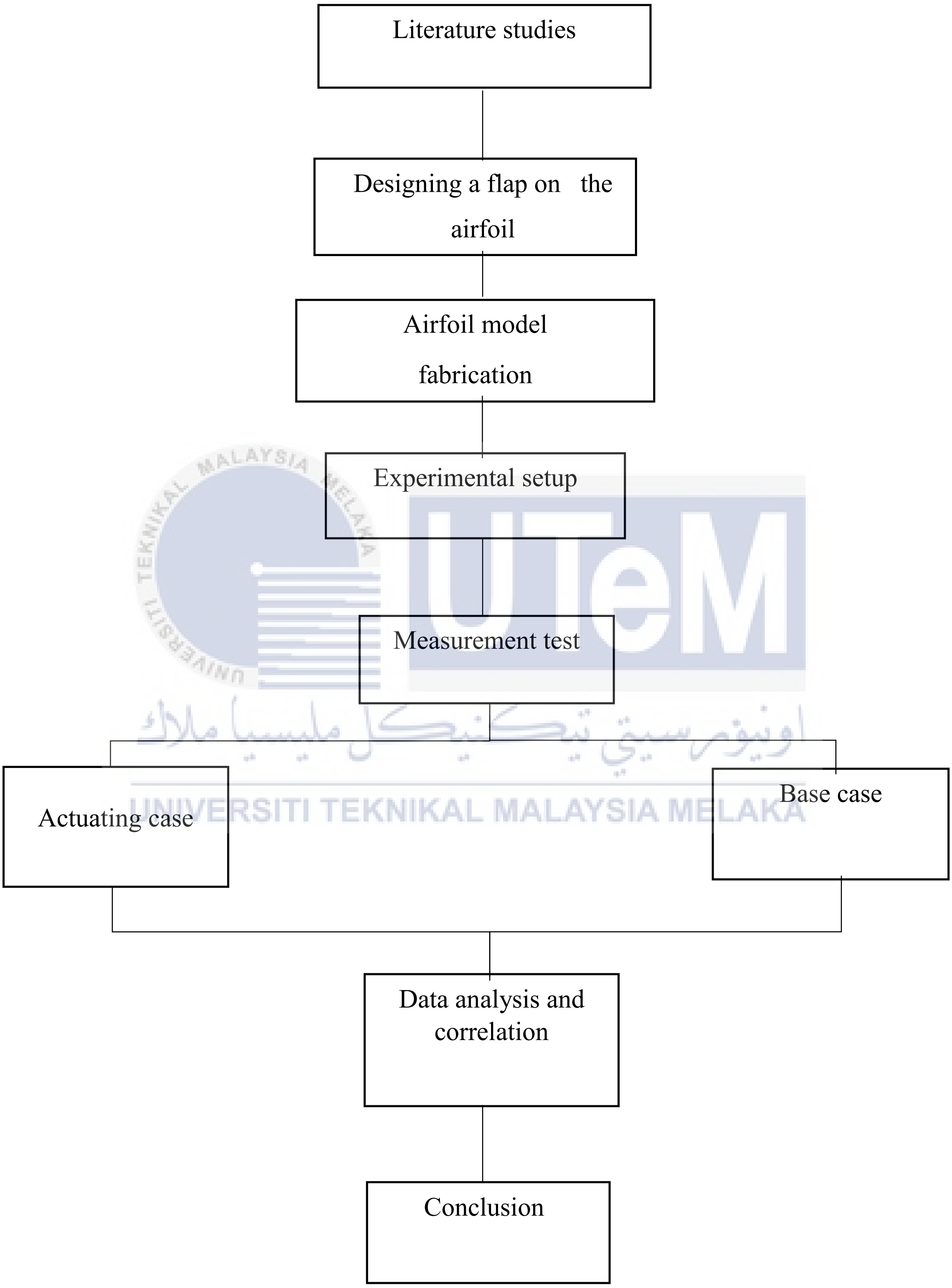

Figure 3 : Flow chart of the experimental step

CHAPTER 2

LITERATURE REVIEW

2.1 OVERVIEW

Literature review is focused on previous study in the related field to obtain knowledge and information for the present study. In this chapter, journals and technical reports from other researchers are selected to be reviewed. The results obtained from the previous study will be compared.

2.2 NUMERICAL AND EXPERIMENTAL INVESTIGATIONS OF LIFT AND DRAG PERFORMANCES OF NACA 0015 WINF TURBINE AIRFOIL BY ADEM ACIR et al. (2015)

In the present work, we studied numerical and experimentally analysis lift and drag performances of NACA 0015 airfoil at different attack angle at low Reynolds numbers (Re) by measuring the forces every two degrees from 0° to 20°. The experiment test was conducted in low speed wind tunnel, and the numerical analysis was performed using CFD program which was FLUENT. The results obtained from experiment and numerical were compared. In this study, stall angle depended on turbulent occurred behind airfoil was determined. As result, effect of the stall angle of airfoil performance was investigated. Experimental investigations are very important due to accuracy. However, those take much time and economic and whenever we want to change a parameter about our study, it is very difficult because of time and economic.

Fortunately, investigators can study very fast and easily thanks to computational fluid dynamics (CFD) programs. These programs can give as correct results as experimental methods. Also, CFD programs can be contributed as regards time and faster according to experimental methods. NACA airfoil types were investigated in the literature. Generally, a lot of investigators studied lift and drag performances of NACA airfoil. Bhat *et al.*, studied oscillating of NACA 0012 airfoils at around stall angle at low Reynolds number. Benard *et al.*, have investigated on the enhancement of the air foil performance by using a plasma actuator in steady and unsteady models.

The authors investigated lift, drag performances and surface pressure by changing attack angle using different turbulence model. In the present work, the lift and drag performances of NACA 0015 wind turbine airfoil were investigated as numerical and experimentally. Also, different turbulence models were performed. Obtained numerical results were compared with experimental results.

2.2.1 Methodology

The measurements have been conducted in an open wind tunnel at the University of Gazi, Faculty of Technology. This tunnel test section long is about 0.4m long and flow cross section is approximately 0.3m×0.3m, interval of wind velocity is from 3.1 to 28 m/s as shown in Figure 4 and Figure 6. The airfoil used in the present study is an academic NACA 0015 profile as shown in Figure 4 (chord length, c, of 100 mm and spanwise length, s, of 100 mm). Stationary end plates are kept on the two sides of the airfoil, with a small gap of about 1 mm, to help maintain two dimensionality of the flow. The experiments has been conducted at 10 m/s wind velocity (V) in tunnel which is corresponding to 68490 Reynolds number (Re).

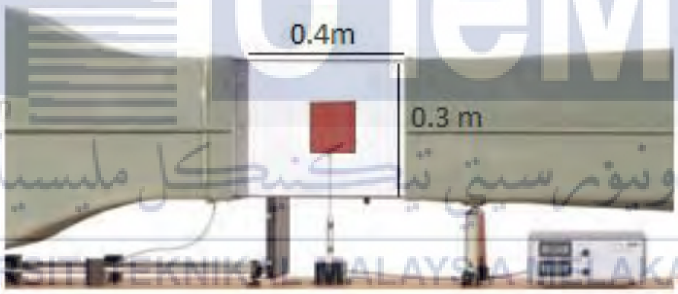

Figure 4 : Wind tunnel test area

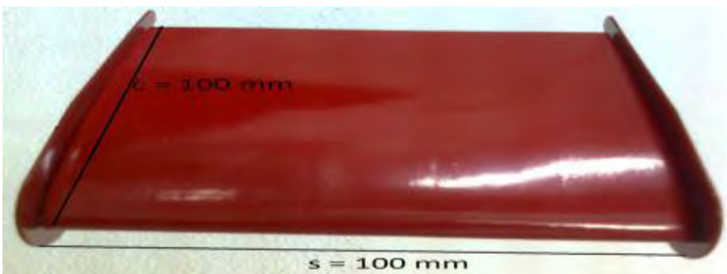

Figure 5 : Airfoil details

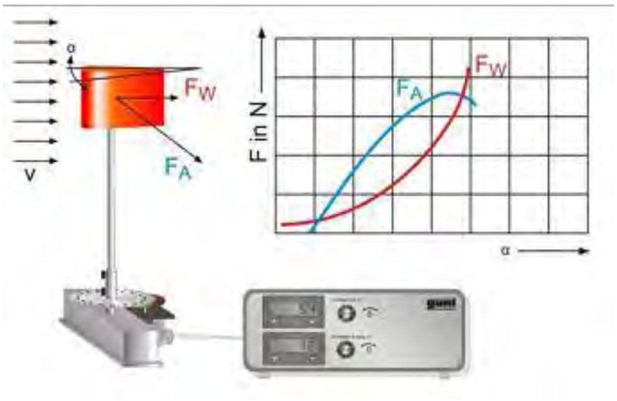

Figure 6 : Wind tunnel test mechanism

The airfoil is forced stationary wind velocity to learn lift and drag coefficient, the airfoil profile is attached to electronic two- component coefficient transducer. The values for drag and lift are displayed digitally on the measurement amplifier. The angular position of the airfoil (angel of attack at airfoil) in the flow is set by means of a graduated dial.

2.2.2 Results

In this study, experimental and numerical analyses were performed. The experiments were conducted at 10 m/s wind velocity (V). Lift and drag coefficient of NACA 0015 airfoil at different attack angle between 0° and 20° were measurement. Also, the lift and drag coefficient were obtained as numerical with FLUENT programs for the same conditions. In numerical analysis C mesh used as shown in Figure 7 and Figure 8. The top bottom and left boundaries were placed at a distance of 10 chords from airfoil whereas the right boundary was placed at 20 cords. A mesh independence study was performed to verify that the solution would not change subsequent additional refinements and 33600 grids number suitable for our model. Airfoils have various shape and sizes.

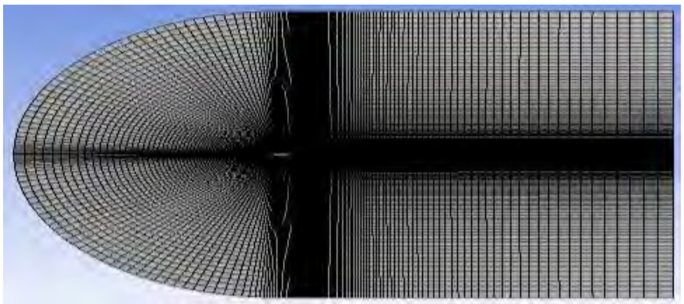

Figure 7 : Structure of C mesh using numerical analysis

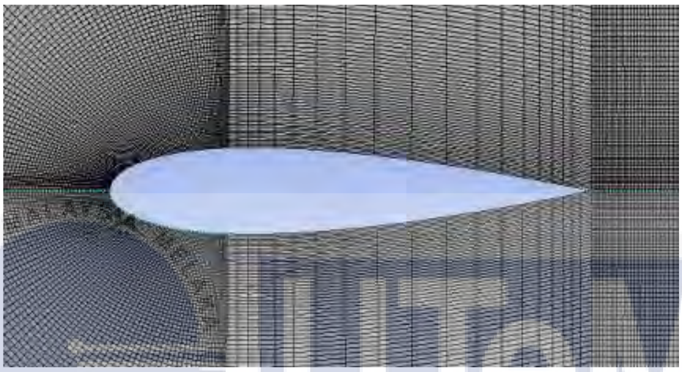

Figure 8 : Mesh around the airfoil

The lift and drag coefficient at wind tunnel test for NACA 0015 airfoil were measured as experimentally. The maximum lift and drag coefficient were found as 0.75 and 0.15 for 16° attack angle. The lift and drag coefficient was primarily effected by attack angle as regards both increasing and decreasing. If attack angle increased, lift and drag coefficient could increase until a certain angle. After the certain angle, the lift coefficient was decreasing whereas; and drag coefficient was increased. This situation was called as stall angle. The stall angle caused transition from laminar to turbulence flow. Also, the lift and drag coefficient were computed with CFD analysis which was used Spalart Allmaras and K-epsilon.

The Spalart Allmaras, K-epsilon and experimental results were compared. Two methods were compared with experimental results. Spalart Allmaras numerical solution method results have better than K-epsilon. Spalart Allmaras method showed similarity experimental results. The flow was laminar around the NACA 0015 airfoil between 0° to 14° angle of attack. Laminar flow was transition turbulence flow and pressure distribution changed around 16° angle of attack so lift coefficient began decrease.

2.3 RANS SIMULATIONS OF AERODYNAMIC PERFORMANCE OF NACA 0015 FLAPPED AIRFOIL BY SOHAIB OBEID et al. (2016)

An analysis of 2D subsonic flow over an NACA 0015 airfoil with a 30% trailing edge flap at a constant Reynolds number of 106 for various incidence angles and a range of flap deflections is presented. The steady-state governing equations of continuity and momentum conservation are solved combined with the realizable k-" turbulence model using the ANSYS-Fluent code (Version 13.7, ANSYS, Inc., Canonsburg, PA, USA). The primary objective of the study is to provide a comprehensive understanding of flow characteristics around the NACA 0015 airfoil as a function of the angle of attack and flap deflection at Re = 10^6 using the realizable k-" turbulence model. The results are validated through comparison of the predictions with the free field experimental measurements. Consistent with the experimental observations, the numerical results show that increased flap deflections increase the maximum lift coefficient, move the zero-lift angle of attack (AoA) to a more negative value, decrease the stall AoA, while the slope of the lift curve remains unchanged and the curve just shifts upwards. In addition, the numerical simulations provide limits for lift increment ΔC_l and $C_{l,max}$ values to be 1.1 and 2.2, respectively, obtained at a flap deflection of 50°. This investigation demonstrates that the realizable k-ε turbulence model is capable of predicting flow features over an airfoil with and without flap deflections with reasonable accuracy.

Recently, there has been considerable interest in flow control, especially in the field of aerodynamics with the intent of increasing lift and decreasing the drag of airfoils. To allow landing and take-off from short runways at reduced ground speeds, some modern airplanes are equipped with multi-element high-lift devices that generate the required high lift. Slat and single or multiple flaps are typical examples of such devices. Multi-element wing designs, however, are found unfavourable from a weight and complexity point of view. That is the reason for replacing the multi-element flap with a single-hinged flap in the current designs to reduce the complexity while increasing the efficiency of the wing. While reducing the complexity of the wing, the single-hinged flap increases the chance for flow separation on the flap at large deflection angles. To prevent or at least to minimize the effects of flow separation, the air flowing over the wing near the surface must be energized so that it could overcome the effects of the adverse pressure gradient encountered along the flap.

An analysis of the flow over the NACA 0015 airfoil with zero flap deflection is first presented. The details of the mathematical model, meshing schemes utilized and the computational analyses are described. This is followed by simulations of flapped airfoils. Validations of the computational results for cases with and without flap deflection are also presented. It is concluded that the realizable k-ε turbulence model is capable of capturing the flow conditions over the airfoils with and without flaps with reasonable accuracy.

2.3.1 Methodology

2.3.1.1 Formulation

In this study, the ANSYS-Fluent (Version 13.7) code is used as the solver along with the realizable k-ε turbulence model for solving the Reynolds Average Navier–Stokes (RANS) equations for flow around the NACA 0015 airfoil with and without a hinged flap. The code solves the equations of the conservation of mass and balance of momentum. Additionally, the transport equations are also solved for turbulence properties.

2.3.1.2 Evaluation of C_p, C_l and C_f

The pressure coefficient, C_p, and the lift coefficient, C_l, are evaluated as,

$$C_p = \frac{p - p_\infty}{q_\infty} \qquad (1)$$

In these equations, p is the surface static pressure; p_∞ is the free stream static pressure; q_∞ is the free stream dynamic pressure, which is defined as $q_\infty = \frac{1}{2}\rho v_\infty^2$ and x/c is the normalized chord-wise position. The skin friction coefficient C_f is the ratio of the surface shear stress, τ to freestream dynamic pressure. That is,

$$C_f = \frac{\tau}{q_\infty} \qquad (2)$$

2.3.1.3 Computational Domain and Boundary Conditions

To facilitate the grid generation process, as well as the analysis, similar to the earlier study of Hassan, the airfoil with the deflected trailing edge flap is treated as a single-element airfoil with no gap between the flap's leading edge and the base of the forward portion of the airfoil. For deflecting the flap, solid body rotations were assumed, and a four-point spline smoothing was made for the resulting airfoil at the chord-wise position corresponding to the location of the flap hinge point. Figure 9 shows the schematic geometry of the NACA 0015 with various trailing edge flap deflections.

Figure 9 : Geometry of the NACA 0015 airfoil with a 30% trailing edge deflected flap

To develop a high efficiency simulation, a C-structured grid topology of a semi-elliptical shape with semi-major diameter 43.5 c and semi-minor diameter 10 c, where c is the chord length, was generated using the pre-processor Gambit. The elliptic shape of the grid provides major advantages over other conventional shapes, such as rectangular and semicircle upstream and rectangular downstream. The main advantage is providing flexibility in using the same mesh for different angles of attack by only shifting the tail part of the mesh at the airfoil trailing edge in accordance with the specific angle of attack. For this purpose, it is made sure that the edge of the elliptic domain has sufficient vertical length to contain the incoming flow for angles of attack up to 20 degrees. The approach also leads to considerable reduction in the needed number of cells in the mesh in the far-field; thus allowing for the majority of the cells in the mesh to be concentrated around the airfoil.

The distance of the rear pressure far field from the airfoil is 30 c, and the majority of the cells are clustered toward the airfoil surface. This sufficiently large domain was chosen to cover flow disturbances created by the airfoil and avoid unphysical reflections from the outer edges of the grid. The schematic of the computational domain and mesh around the airfoil is shown in Figure 10.

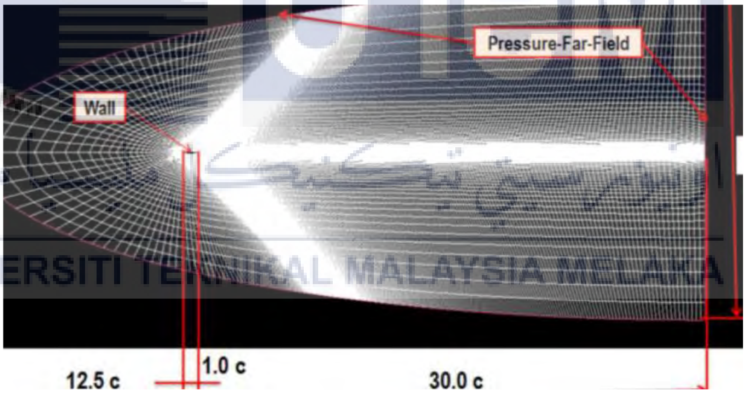

Figure 10 : Domain of calculations and boundary conditions.

2.3.1.4 Setting up of the Numerical Simulation Parameters

Time independent pressure-based solver is used within ANSYS-Fluent for the analysis. The realizable k-ε turbulence model is selected for analyzing the boundary layer flow over the airfoil. The airflow is assumed to be incompressible. A simple scheme with the Green-Gausscell-based gradient implicit formulation of pressure velocity coupling is utilized. For spatial discretization, the second order upwind differencing scheme which offers several advantages over a central-differencing formulation for computing viscous flows is used in this work. The ANSYS-Fluent code solves the coupled governing equations of fluid motion simultaneously and provides updating correction for the pressure value in each iteration. A convergence criterion of 1 x 10^8 was used for the continuity, x-velocity, y-velocity, k and ε. All solutions converged with the standard interpolation scheme for calculating cell-face pressure and second order up-wind density, momentum, turbulent kinetic energy, turbulent dissipation rate and energy interpolation schemes for turbulent flow.

2.3.2 Results

2.3.2.1 NACA 0015 Airfoil with Zero Flap Deflection

Figure 11 shows the variation of the lift-to-drag ratio (C_l/C_d) with the incidence angle as predicted by the realizable k-ε model and the comparison with the available experimental data and earlier simulations. It is seen that the lift-to-drag ratio increases rapidly from zero at α = 0° toward its maximum value with the increase in incidence angle. This is because for small angles of attack, both C_l and C_d increase, but C_l increases faster than C_d. Then, as the angle of attack further increases, the lift-to-drag ratio decreases, and the decreasing trends are continuous to beyond the stall angle.

While the trend of variations of the lift-to-drag ratio of the present simulations is in qualitative agreement with the experimental data and earlier simulations, there are quantitative differences in the peak value of this ratio. The maximum value of lift-to-drag ratio found for the present simulations is 48.2, which occurs at AoA of 8.5°.

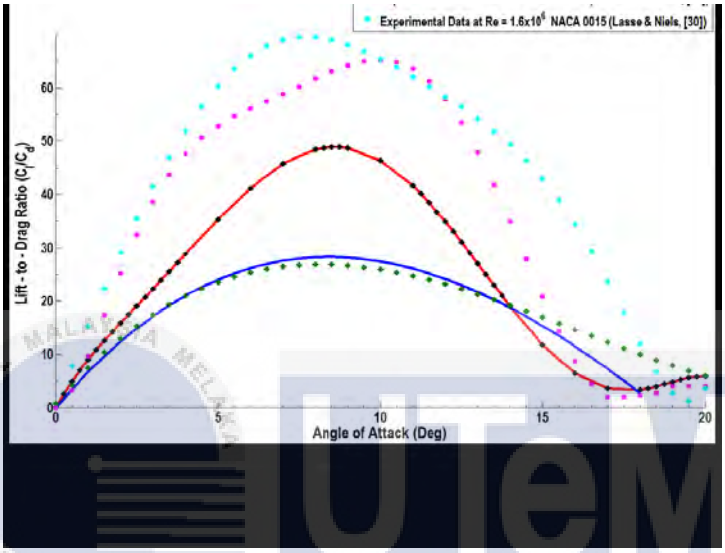

Figure 11 : Comparison of the lift-to-drag $\frac{C_l}{C_d}$ ratio of the airfoil at 0° flap deflection versus the angle of attack at chord Re = 10^6 with experimental data and earlier numerical

2.3.2.2 NACA 0015 Airfoil with Flap Deflection

The effect of downward flap deflection on the aerodynamic performance of the airfoil is studied for eight different flap positions of 2°, 5°, 10°, 15°, 20°, 25°, 30° and 40°. The comparison of the static pressure contours for zero flap deflection and for the deflected flap at the same angle of attack shows that the flap deflection increases the negative pressure over the entire upper surface of the main airfoil and increases the positive pressure on the lower surface near the trailing edge. The pressure on the lower surface increases rapidly with flap deflection, while the pressure on the upper surface increases gradually. The pressures on both the upper and the lower surfaces of the flap increase with flap deflection.

The turbulence intensity contours of the flow around the flapped airfoil at some selected deflection angles and zero incidence are also evaluated. It is observed that at the zero incidence angle, the flap deflection has a pronounced influence on the turbulence intensity around the flapped airfoil. Even a small deflection in flap angle disturbs the flow and creates regions of high turbulence intensity in the upper surface of the flapped airfoil. These regions expand with increasing of the flap deflection and shift from the main airfoil towards the flap section. However, the maximum turbulence intensity occurs in the wake region close to the flap in addition to the boundary layer regions. This is due to the fact that the region with recirculating flow becomes larger as the wake width increases with the flap deflection. At high flap deflections, the flow separates from the flap, and high pressure acting on the pressure side of the flapped airfoil and consequently marked increase in the drag occur compared to situations where the flow remains attach to the surface.

2.4 INFLUENCE OF INFLOW ANGLE ON FLEXIBLE FLAP AERODYNAMIC PERFORMANCE BY H Y ZHAO et al. (2007)

Large scale wind turbines have larger blade lengths and weights, which creates new challenges for blade design. This paper selects NREL S809 airfoil, and uses the parameterized technology to realize the flexible trailing edge deformation, researches the dynamic aerodynamic characteristics in the process of continuous flexible deformation, analyses the influence of inflow angle on flexible flap aerodynamic performance, in order to further realize the flexible wind turbine blade design and provides some references for the active control scheme. The results show that compared with the original airfoil, proper trailing edge deformation can improve the lift coefficient, reduce the drag coefficient, and thereby more efficiently realize flow field active control. With inflow angle increases, dynamic lift-drag coefficient hysteresis loop shape deviation occurs, even turns into different shapes. Appropriate swing angle can improve the flap lift coefficient, but may cause early separation of flow. To improve the overall performance of wind turbine blades, different angular control should be used at different cross sections, in order to achieve the best performance.

At present, the flexible structure research mainly focuses on smart morphing wings in the field of aerospace, in the field of wind turbine blades basically focuses on material, structural performance and control institutions. Since Andrew systematically applied smart flexible structure in 50 kW blade for the first time, the study of flexible blade is always based on the joint design of bending and twisting with airfoil structure not changed, active flexible flap airfoil research suggests that appropriate flexible deformation can improve aerodynamic performance. Wind turbine blade is made of airfoil sections with different chord lengths and twist angles and different cross sections have different angles of attack, this article selects specific inflow angles to study the flap aerodynamic characteristics.

We select NREL S809 airfoil, using the parameterized technology to achieve its flexible trailing edge deformation, study the influence of inflow angle on flexible flap aerodynamic characteristics and transition point, provide some references for further realize the flexible wind turbine blade design and the active control scheme.

2.4.1 Methodology

2.4.1.1 Deformation mechanism

Take NREL S809 airfoil as the original airfoil, define H point on the chord line as the hinge point, the part backward swings up and down around that point, keeping the chord length and thickness unchanged. The profile is determined by the Bezier interpolation. With the inflow velocity U_∞ direction keeping unchanged, then the angle of attack α_t increases when the trailing edge (T) swings down, so define the swing angle (the angle between the attachment of H point and T point and the original chord line at any time) is positive when the tail rotates clockwise from the original position.

2.4.1.2 Meshing and calculation conditions

We used reforming dynamic mesh technique; the flow field calculation domain is shown in Figure 12, the mesh distribution is shown in Figure 13, the upstream inflow zone is a semicircle of $r = 10c$, the dynamic grid zone is a circular region of $r = c$, the downstream wake zone is a square of $20c$ x $20c$. Control equations: static aerodynamic characteristics calculation used potential flow equation coupled with the boundary layer equation, the dynamic aerodynamic characteristics calculation used the RANS equation and k-ε turbulence model, inflow Reynolds number Re = 8 x 10^5.

Boundary conditions: inlet velocity, pressure outlet, no slip wall condition is used on airfoil surface. Swing angle control: the initial angle is 0°, flexible tail swing period is 2s and time step is 0.01s, angular range is -25°~25°. Flap parameters: NREL S809 airfoil as original airfoil, take 0.750*c* as hinge point. Inflow angles: select -5°, 0°, 5°, 10° as inflow angles for flexible flap numerical simulation

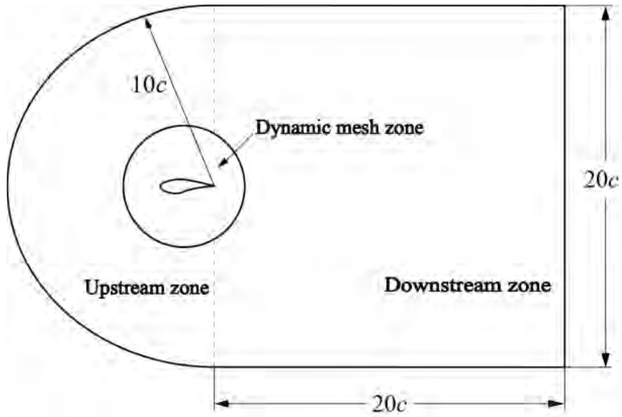

Figure 12 : Flow field calculation domain

Figure 13 : Calculation domain mesh

2.4.2 Result

Dynamic lift-drag characteristics were analysed with changing of angle of attack, swing angle and flow time below. The closed curve is dynamic lift-drag coefficients of flap, the open curve is static lift-drag coefficients of S809 original airfoil. Comparing the static and dynamic lift-drag characteristics, it can be found that the dynamic process of the flap makes its lift-drag coefficients do not change along the static curve, which on the one hand is due to the dynamic response of the process has obvious hysteresis phenomenon to time, on the other hand is due to with the same actual angle of attack, the swing angle change leads airfoil camber to change, thus influence the aerodynamic characteristics.

Comparing flap dynamic process at different inflow angles, it can be found that with the increase of Φ starting from zero, the flap lift coefficient increases overall, to $\Phi = 5°$ the curve flips from ○ shape to ∞ shape, continually increase to 10° almost turn to a reversed type. At $\Phi = -5°$ and $\Phi = 5°$ the shape and position of dynamic drag coefficient closed loop with the angle of attack offsets from that at $\Phi = 0°$. At $\Phi = 10°$ the drag coefficient increases sharply, which is due to the separation of the flow.

Figure 14 is a pressure contour and flow chart around the flap under different inflow angles with 25°. As can be seen from Figure 14(a), although the inflow angle is -5°, the flap still has its lower side surface as the pressure side and the upper side surface as the suction side, that is because the flap swing angle is 25°, resulting a positive actual angle of attack for the flap, we can intuitively see the actual angle of attack is about 1.2°. Inflow angle increases from -5° to 5°, the pressure difference between upper and lower surface of flap gradually increases, when inflow angle increases to 10° the pressure difference is reduced, this is because the flow has been in a serious separation. Flow in Figure 14(c) has separated, the flap may cause flow early separation at the same time while increasing the lift coefficient.

(a) Φ = -5°

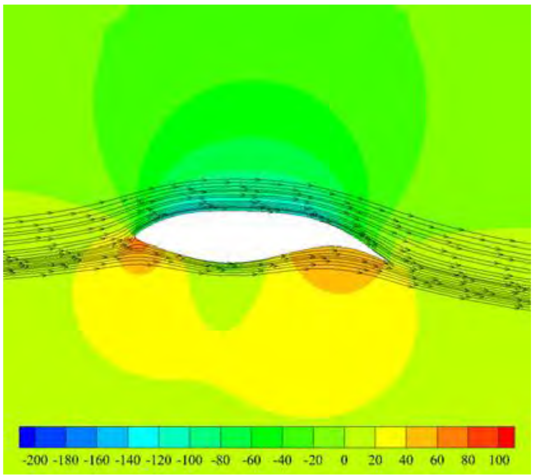

(b) Φ = 0°

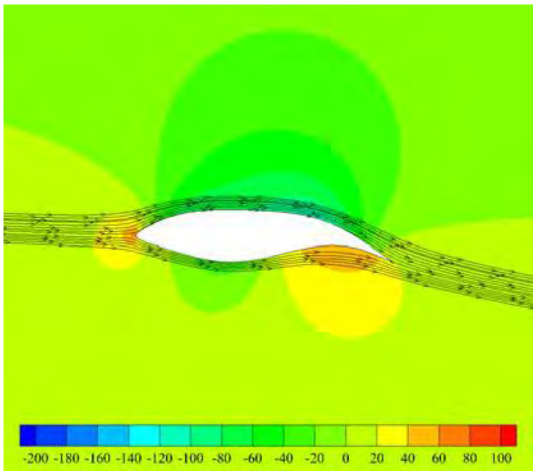

(c) Φ = 5°

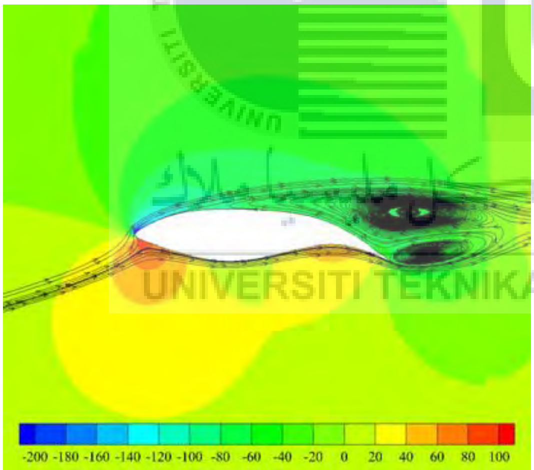

(d) Φ = 10°

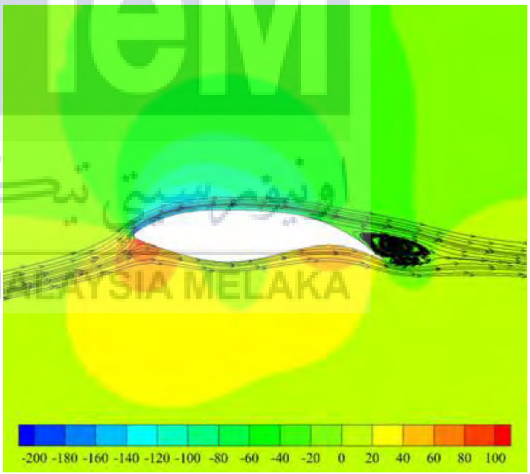

Figure 14 : Pressure contour and flow chart around the flap under different inflow angles

2.5 INVESTIGATION OF THE EFFECT OF TUBERCLES ON AIRFOIL PERFORMANCE BY JARED CARR et al. (2014)

The effect of tubercles on the leading edge of a NACA 0020 airfoil section was investigated numerically and experimentally. The motivation for this experiment was to explore the ways in which airfoil performance can be improved by modifying the contour of the leading edge. Lift and drag coefficients between a standard NACA 0020 airfoil and one with a sinusoidal shaped leading edge were compared under a constant wind speed of 33.5 mph and angles of attack ranging from 0° to 20°. It was found that the airfoil with leading edge tubercles stalled at a 14° angle of attack with a maximum lift coefficient of 0.48, which was earlier than the standard airfoil stall angle of 16° at a maximum lift coefficient of 0.65. However, the airfoil with tubercles experienced a more gradual decline in lift coefficient after stalling compared to the standard airfoil. These effects may help aircraft attain greater maneuverability at high angles of attack and more stable post-stall behavior.

Tubercles affect the behavior of an airfoil at near-critical angles of attack. The unevenness of the leading edge channels the fluid into narrower and faster moving streams. These protrusions energize the previously laminar flow and allow the boundary layer following the leading edge troughs to stay connected to the airfoil surface at higher angles of attack, much like vortex generators on an aircraft wing. Therefore, unlike the standard airfoil, detachment of the boundary layer occurs at different angles for different points along the wingspan, resulting in a more gradual overall decrease in lift coefficient at stall. With this observation come many implications. Reduction in the abruptness of the drop in lift may provide a way to reduce the dangers associated with sudden changes in the force on the airfoil. Stalling most frequently occurs during aircraft liftoff and landing during which the angles of attack are usually the greatest and closest to the critical angle.

Moreover, stalling is also most dangerous during these instances because the aircraft is close to the ground and has little space to correct for the effects of stalling. Tubercles have the potential to mitigate this danger by increasing controllability of the aircraft should stalling effects take place. Another advantage of having tubercles is the increased manoeuvrability as a result of the more gradual stall response. Observation of humpback whale fins has shown that leading edge tubercles appear to allow for greater 3-dimensional agility when the whales hunt for prey. In this light, aircrafts have the potential to be designed to move with more freedom and built with fewer structural constraints. This experiment was designed to characterize the effects of airfoil tubercles and determine the feasibility of applying this technology in aerospace engineering. The main focus is the comparison of lift coefficients at various angles of attack, location of stall angle, and the rate of change in lift coefficient for the angles of attack following the stall angle.

2.5.1 Methodology

2.5.1.1 Apparatus

A subsonic wind tunnel was used to determine the lift and drag for the two airfoils at varying angles of attack. The wind tunnel consists of three sections: nozzle, test section, and exit. Air enters a 9:1 contraction cone of the nozzle, which is screened by a honeycomb filter to decrease turbulence of the air entering the test section. This contraction cone is followed by the straight test section with the dimensions of 1” x 10” x 36” (height x width x length) in which the airfoils were mounted. The exit consists of an air outflow and a motor-driven fan whose speed is controlled by a frequency drive. A Monarch optical tachometer provides real-time measurements of the fan rotor speed. The maximum wind speed inside the test chamber that the fan-motor can generate is approximately 55 mph at the peak motor RPM. The contraction cone is fitted with a Dwyer pitot-tube paired with an Omega pressure transducer to measure the pressure drop across the entry into the test section.

Lift and drag forces were calculated independently throughout the course of the experiment using the voltage readings from a strain gauge tower. The strain gauge tower features an Omega strain gauge that is capable of determining strain in a single direction. Force data were collected in orthogonal directions and transformed into lift and drag in post-processing using a MATLAB script. The strain gauge schematics are illustrated in detail below in Figure 15. Additionally, a smoke wand and camera were used to visualize the airflow past the airfoil at approximately 33.5 mph wind speed.

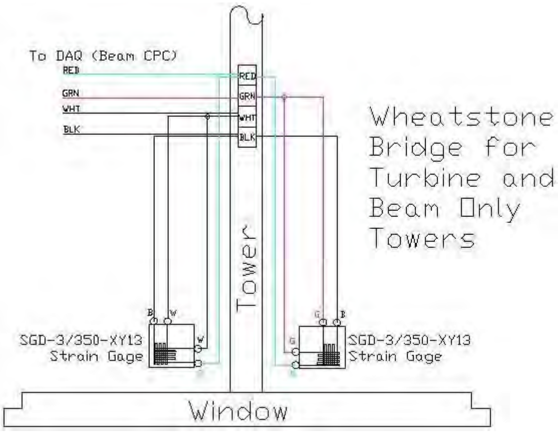

Figure 15 : Strain gauge schematics

The two airfoil prototypes were 3D-printed using an SST 1200ES Fused Deposition Modelling Machine, which uses a soluble support material and ABS+ polymer for the model material. The printer has a maximum resolution of 0. 5mm (0.010”), 0. % of the nominal chord length. Both airfoil models have a span of 7 inches and a mean chord line of 5 inches. The sinusoidal contour of the leading edge tubercles has a wavelength of 2.1 inches and amplitude of 0.222 inches from peak to peak. The weight of the standard NACA 0020 airfoil (Figure 16) and NACA 0020 airfoil (Figure 17) featuring leading edge tubercles are 300.1 grams and 132.8 grams respectively.

Figure 16 : 3D CAD Model of standard NACA 0020 Airfoil

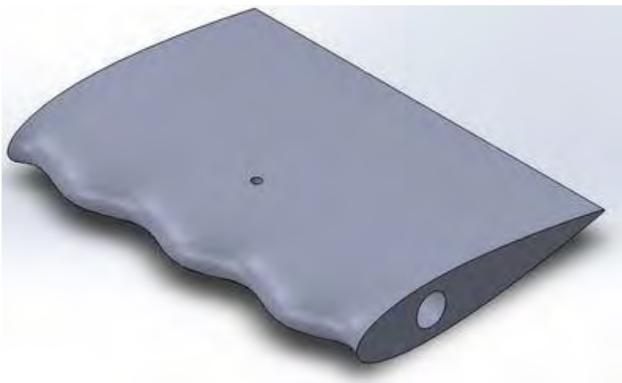

Figure 17 : 3D CAD Model of NACA 0020 Airfoil Modified with Tubercles

2.5.1.2 Mathematical Model

The following analytical model describing the effect of tubercles on a symmetric (under cambered) airfoil makes use of the following standard aerodynamics assumptions:

- Incompressible working fluid (air) at these low airspeeds
- Large Reynolds number flow
- Large aspect ratio wing

Incompressible flow assumption is valid because the airspeed is much lower than the Mach 0.3 critical airspeed between incompressible and compressible regimes. The large Reynolds number flow assumption derives from the calculated Reynolds number of 1.3 x 10^5. The last assumption is valid because the airfoil spans the majority of the section of the wind tunnel. Thus, the baseline NACA 0020 airfoil can be analyzed assuming 2-dimensional flow. It is only with the addition of tubercles that 3D effects must be considered. Using XFoil simulation software, it was found that for a theoretical NACA 0020 airfoil, stall occurs at 14°. Thus, consistent with assumptions made earlier, the local critical angle will be slightly higher on the cross-section of the trough, and slightly lower for the crest than this theoretical value.

2.5.2 Result

2.5.2.1 Performance of Standard Airfoil

Before the airfoil with tubercles could be tested and analyzed, a baseline must be established for comparison. To do so, a standard NACA 0020 airfoil was tested in the wind tunnel with wind speed of 33.5 MPH and angles of attack ranging from 0° to 20°. By using the lift and drag force data acquired from converting the strain gauge voltage reading into the necessary force readings, the lift and drag coefficients were calculated.

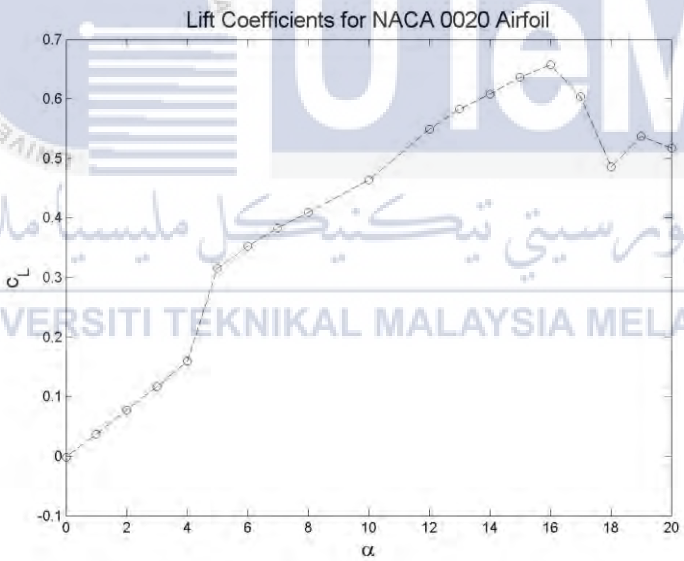

Figure 18 : Lift coefficient vs angle of attack, standard NACA 0020 airfoil

Figure 18 above indicates that the standard airfoil experienced stall at an angle of approximately 16°, with a maximum coefficient of lift of 0.65. To visualize the separation, the smoke wand was used to generate a visible stream over the airfoil. When the airfoil was rotated to angles of attack greater than 16°, greater degrees of boundary layer detachment were observed. Note that in order to mitigate wall effects, a negative angle of attack was used, giving more room to deflected streamlines above the model.

2.5.2.2 Performance of Airfoil with Tubercles

As shown in Figure 19, the modified airfoil differed from the standard airfoil in several key aspects. First, the lift coefficient for the NACA 0020 airfoil with tubercles peaks at a stall angle of 14°, earlier than the previously determined stall angle of 16° for the standard NACA 0020 airfoil. This suggests the tubercles are ineffective in delaying stall, as there is a marked decrease in performance compared to the standard airfoil. Pre-stall behavior is almost identical between the two airfoils, featuring a similar rate of gain in lift as the angle of attack increased. Despite this, the maximum lift coefficient achieved by the modified airfoil is only 0.48, lower than the 0.65 of the standard airfoil.

However, because there was a sudden jump in the lift data of the standard airfoil, conclusions concerning the true maximum lift coefficient cannot be confidently made. As a tradeoff for this loss of performance in the pre-stall and stall regimes, the post-stall behavior of the modified airfoil benefited from a more gradual decrease in lift coefficient. Instead of a sudden drop in lift coefficient once the stall angle is exceeded, seen by the drop from a lift coefficient of 0.65 at an angle of attack of 16° to a lift coefficient of 0.47 at an angle of attack of 18° for the standard airfoil, the lift coefficient for the modified airfoil only drops from 0.48 to 0.40 from an angle of attack of 14° to 18°. This demonstrates that in the post-stall regime airfoil performance is greatly stabilized with the addition of tubercles. Hansen et al. noted the same behavior for a NACA 0021 airfoil modified with tubercles, confirming that tubercles aid the post-stall behavior of an airfoil at the cost of decreased pre-stall and stall performance, at least for symmetric airfoils of a similar shape.

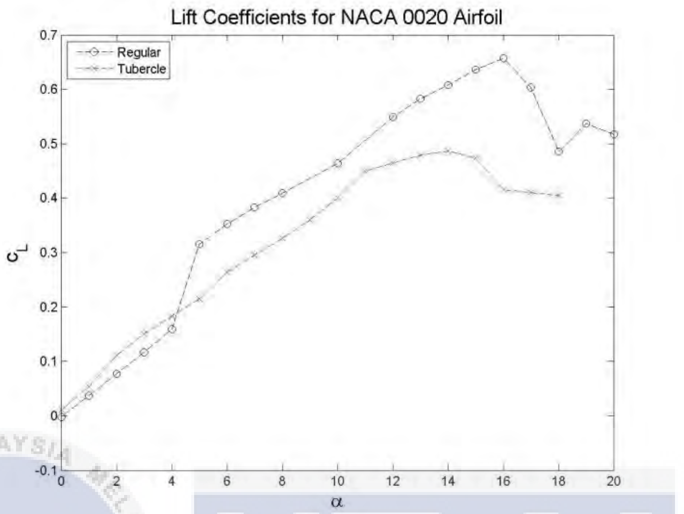

Figure 19 : Lift coefficient vs angle of attack, NACA 0020 airfoil with tubercles vs. unmodified airfoil

2.6 CONCLUSION

This chapter describes some of the studies that have been done by some people about the differences between the airfoil with an airfoil with flap and no flap. These data are important are described in this chapter as a reference for this study. There are various methods to study the drag and lift coefficient, and the easiest way is to use a wind tunnel. In addition, based on the literature review that was done, the wind tunnel is used to find various important values such as drag and lift force, pressure distribution, dynamic pressure, static pressure, and so on. A wind tunnel is a tool used in aerodynamic research to study the effects of air moving past solid objects.

A wind tunnel consists of a tubular passage with the object under test mounted in the middle. Air is made to move past the object by a powerful fan system or other means. The test object, often called a wind tunnel model, is instrumented with suitable sensors to measure aerodynamic forces, pressure distribution, or other aerodynamic-related characteristics. Based on the objective, value that needs to be studied are drag and lift coefficient on the NACA 0015 airfoil. Through the use of wind tunnel experiment, the value that can be obtained is drag and lift force so few important formula should be used to achieve the objective of the project.

CHAPTER 3

METHODOLOGY

3.1 OVERVIEW

This section will focus on the data collection through experimental method. The procedures of this experiment, method used, steps for settings and equipment used will be discussed in this chapter.

3.2 INTRODUCTION

An experiments were performed to study the effect of flap to aerodynamics performance of airfoil and to compare the result between the base case and actuating case. Basically, there are three steps to run this experiment which are design the airfoil using a SolidWork software, fabrication of airfoil, and lastly testing the airfoil at the wind tunnel to measure the drag and lift force of a NACA 0015 airfoil.

3.3 FLOW CHART

A flowchart is a type of diagram that represents an algorithm, workflow or process, shows the steps as boxes of various kinds, and their order by connecting them with arrows. This diagrammatic representation illustrates a solution model to a given problem and it is used in designing and documenting simple processes. So for this experimental investigation, this flow chart will show the flow of the methodology process of whole experiment in briefly step by step in Figure 20.

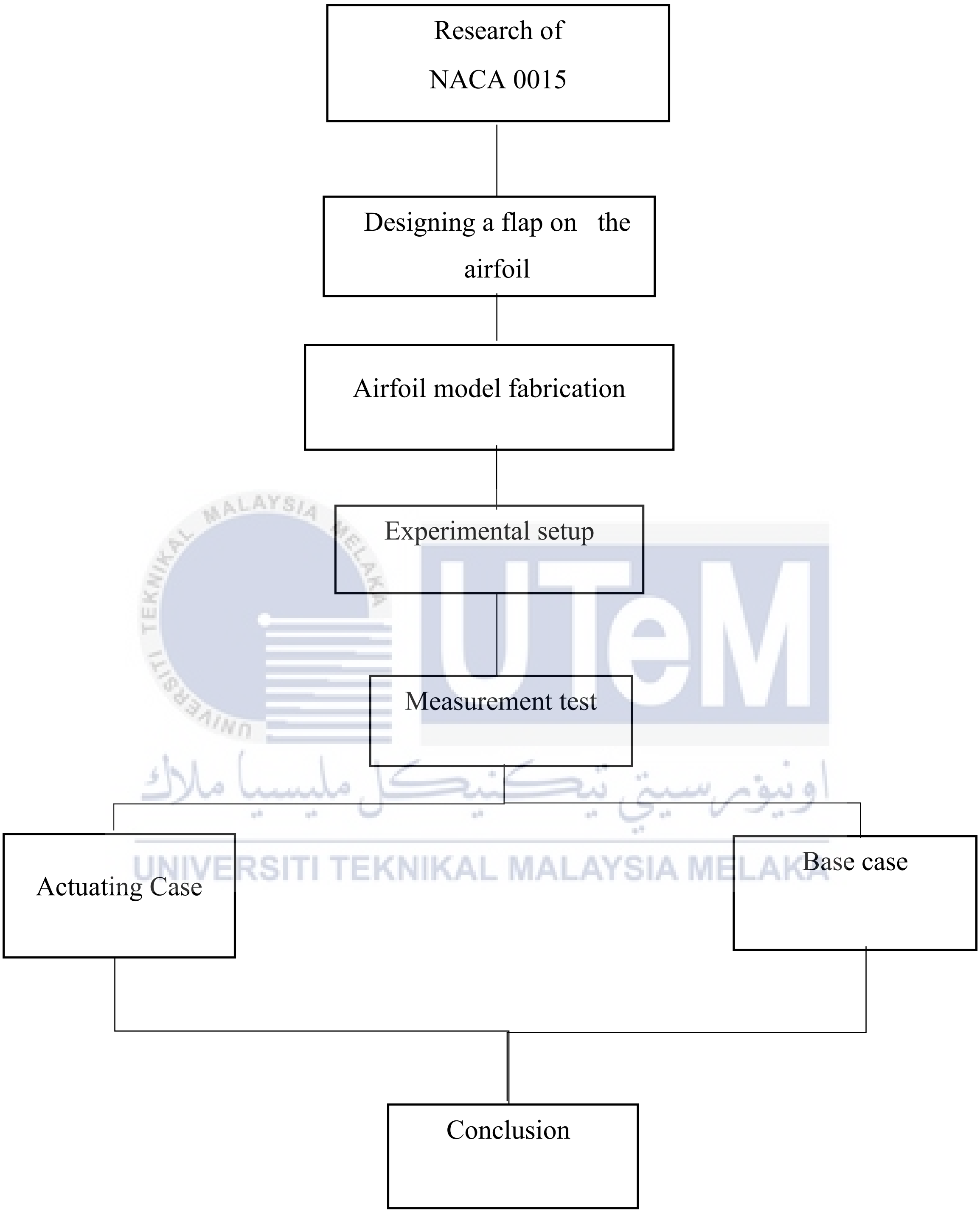

Figure 20 : Flow chart of the methodology

3.4 EQUIPMENT AND MATERIALS

Equipment and materials used in this study are commonly used in the previous study as the set-up of the experiment is quite the same as others. The differences are only in the objective of the study and the specific value that need to be investigated such as air velocity and angle of attack of an airfoil. Basically there are a few equipment that need to be prepared to run this experiment which are 3D printer machine, bench drill machine and wind tunnel. Material selection in this study is only for the printed airfoil which use Acrylonitrile-Butadiene-Styrene (ABS) as shown in Figure 25.

3.4.1 3D Printer Machine

3D printer used in this study is CubePro Duo model 401734 with prints 2.5 times larger than any other desktop prosumer and hobbyist printer (11.2" x 10.6" x 9.06" or 285.4mm x 270.4mm x 230mm) with ultrahigh-resolution settings of 70-micron thin print layers. Besides, the simple set-up process and 25 in-built designs make it incredibly simple for first time users to begin utilising the full capacity and capabilities of the CubePro Duo (Figure 21). The unit works intuitively with Cubify software for iOS and Android devices, allowing the transfer and sharing of images captured and designs created. In addition, it uses a selection of different printing materials, helping to build functional printed objects. Durable but malleable materials including nylon, ABS and PLA can all be used to print intelligent designs.

Figure 21 : CubePro Duo

3.4.2 Bench Drill Machine

Bench drill machine is a drill press in which power transmission from the motor to the spindle is achieved solely through spur gearing inside the machine's head. No friction elements of any kind are used, which assures a positive drive at all times and minimizes maintenance requirements. Gear head drills are intended for metalworking applications where the drilling forces are higher and the desired speed (RPM) is lower than that used for woodworking.

Levers attached to one side of the head are used to select different gear ratios to change the spindle speed, usually in conjunction with a two- or three-speed motor (this varies with the material). Most machines of this type are designed to be operated on three-phase electric power and are generally of more rugged construction than equivalently sized belt-driven units. Virtually all examples have geared racks for adjusting the table and head position on the column. This machine is shown in Figure 22. Basically this machine used to drill the body of an airfoil.

Figure 22 : Bench Drill Machine

3.4.3 Wind Tunnel

Wind tunnel is a tool used in aerodynamic research to study the effects of air moving past solid objects. A wind tunnel (Figure 23) consists of a tubular passage with the object under test mounted in the middle. Air is made to move past the object by a powerful fan system or other means. The test object, often called a wind tunnel model, is instrumented with suitable sensors to measure aerodynamic forces, pressure distribution, or other aerodynamic-related characteristics. Air velocity through the test section is determined by Bernoulli's principle. Measurement of the dynamic pressure, the static pressure, and (for compressible flow only) the temperature rise in the airflow. The direction of airflow around a model can be determined by tufts of yarn attached to the aerodynamic surfaces. The direction of airflow approaching a surface can be visualized by mounting threads in the airflow ahead of and aft of the test model. Smoke or bubbles of liquid can be introduced into the airflow upstream of the test model, and their path around the model can be photographed.

Figure 23 : Wind Tunnel

3.4.4 Prototype of NACA 0015 and its material

This prototype is used during the experiment in the wind tunnel as shown in (Figure 34). The explanation of the flow and steps will be explained later in next subtopic. The material of this airfoil (Figure 24) is ABS as it is manufactured through a 3D printer. Dimensions of this airfoil have been set-up same as NACA 0015 and the chord and span length are 130mm x 130mm.

Figure 24 : A prototype of an airfoil

Acrylonitrile-Butadiene-Styrene (ABS) is a material used for this airfoil. ABS (Figure 25) is an opaque thermoplastic polymer material made from the monomers Acrylonitrile, 1,3-Butadiene and Styrene. Strong and durable even at low temperatures, it offers good resistance to heat and chemicals and is easy to process.

Figure 25 : Acrylonitrile-Butadiene-Styrene (ABS)

3.5 EXPERIMENTS CONDUCTED

3.5.1 Design a NACA 0015 airfoil

Even though there are many choices that can be used to design or create an airfoil, but SolidWork software is the simplest and related to the study. So, the airfoil is designed based on its actual coordinates which is referring to the NACA 0015 coordinates. NACA was the predecessor to NASA and the four digits of the aerofoil name are a code for a series of equations that completely define the shape. The coordinates for this should be available and can be found in internet. Figure 26 shows the coordinates.

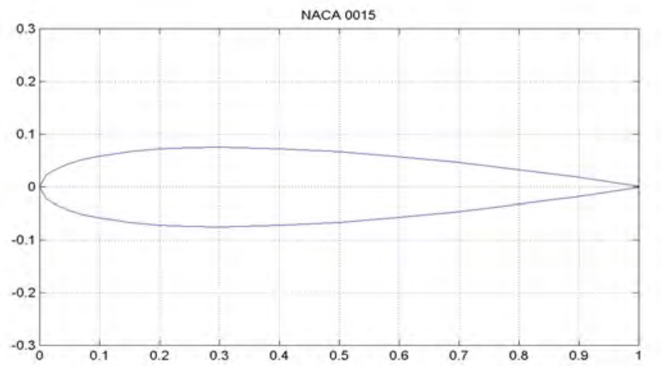

Figure 26 : The coordinates of NACA 0015 airfoil

So, to create a straight and a twisted 3D shape of an airfoil, firstly to make it easier, the airfoil coordinates need to be manipulated by using a spreadsheet program and then export it as a text. Note that the last point in the airfoil coordinates must be the same as the first one so that the coordinates form a loop. Then sketch the airfoil on the selected plane. In addition, the airfoil's design is referring to its own dimensions with a chord length of 130 mm and span of 130 mm. To complete the drawing of an airfoil, there are a few important features in a SolidWork software such as selecting a true plane, convert entities, extrude, curve, sweep and twist. If all of the steps have been done, then the airfoil should end up with something like in Figure 27.

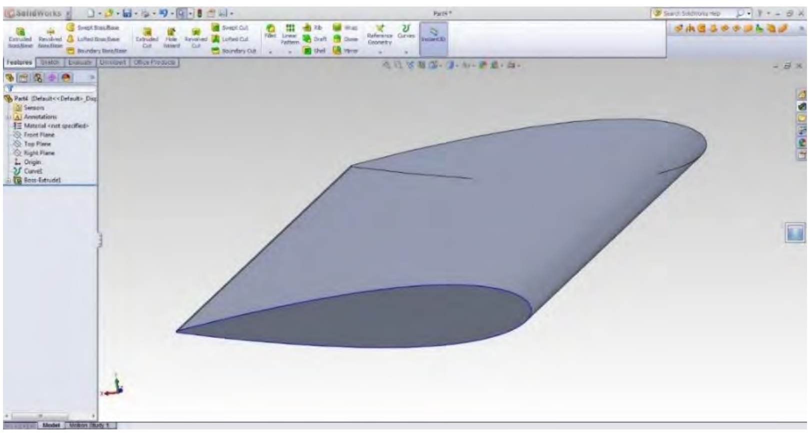

Figure 27 : Drawing of a complete airfoil in SolidWork software

3.5.2 Fabrication of airfoil

In a previous study, there a many ways to construct or fabricate the airfoil such as ultraviolet (UV) Resin, hand layup method, and a vacuum resin infusionor (VRI), which is a process where a vacuum is used to pull resin through dry fabric. In this experiment, a 3D printing machine is chosen as the main method to fabricate the airfoil. This method actually is chosen because UTeM have provide this machine in a mechanical engineering laboratory.

3D printing is part of a process known as preservative manufacturing, where an object is created by adding material layer by layer. Additive manufacturing allows designers to create complex parts for this airfoil at a fraction of the cost and time of standard. Some printers have a removable bioplastic spools in the back of the device almost like a string. When the printer receives the data, it pulls the material through a tube, melts it, and send it to the plate, where it instantly cools. The 3D airfoil is created through layering where the printer will add one layer of the object at a time until it is a fully formed structure. The most common material used in 3D printing is plastic. There are 5 steps in handling this machine:

i. Select and install the suitable material
ii. Synchronize the drawing to the machine using a CubePro software.

iii. Apply a glue on a plate

This glue in Figure 28 is used as a base of the printed object. It will be applied on a plate before the printing is started. Basically, the function of this glue is to avoid any of the material attached to the plate and to make the printer user easier to separate the printed object from the plate after finish printing. When the glue is applied, the heating process is needed to make sure the glue on the plate is fully dry (Figure 29).

Figure 28 : Cube Glue

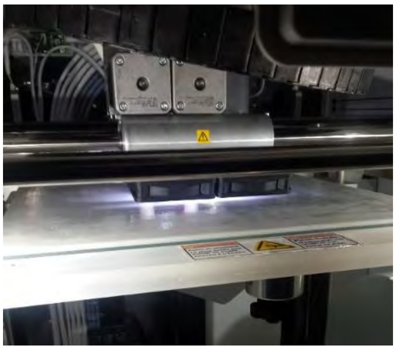

Figure 29 : Heating process

iv. Start the printing

After finish applying glue to the plate, the printing process can be started as shown in Figure 30.

Figure 30 : Printing process

The airfoil formed will be in ABS material and it is a good selected material in order to test this it in a wind tunnel during an experiment. Time taken for the machine to fully produce a printed airfoil is normally around 5 to 6 hours depends on its size. So throughout the printing process is carried out, this machine can only be handled by staff who are in the laboratory only. Steps and procedures to run the machine is very important means not everyone can used it. For slap on the airfoil, it must be printed separately with the body of the airfoil so that we can control the angle of slap easily. The length of the slap is 30mm which the full length of the airfoil is 130mm. The process started with material jetting which material is applied in droplets through a small diameter nozzle, similar to the way a common inkjet paper printer works, but it is applied layer-by-layer to a build platform making a 3D object and then hardened by UV light. Therefore, the bigger size of the model that need to be printed, the longer time taken for the printing process.

v. Finish printing

Time taken to complete the printing process is showed by referring to the printer. Once the process is finish, the model should be slowly scraped from the plate using a scraper (Figure 31). Warm water or tap water should be used to facilitate the material attached to the plate off. The model has been completed can be seen in Figure 32.

Figure 31 : Scrapper

Figure 32 : Body and Flap of the airfoil

The next step is to attach the two parts using a hinge so that its position can be controlled manually. Holes must be drilled using a bench drill first before installing the hinges. Figure 33 shows both parts has been joined by a hinge.

Figure 33 : Full image of the NACA 0015 airfoil

3.5.3 Wind tunnel testing

Aerodynamicists use wind tunnels to test models of proposed aircraft and engine components. The most basic type of instrument is the force balance. The experiment was conducted in the Mechanical Engineering's subsonic wind tunnel located at the Technical University of Malaysia Malacca (UTeM). This is a low turbulence, closed-loop atmospheric wind tunnel capable of tunnel velocities of 40 m/s. A wind tunnel which is a duct contains air flow or other gas. It is usually used to study about the flow past the models of aircraft, structures and vehicles, etc. There are many types of wind tunnels in the world which with different scales. Wind tunnel testing is a pivotal step in the outline of an airfoil. It can give very exact data on the execution of an airfoil or a section of an airfoil by taking information on a scale model. This can save colossal amount of money by testing models instead of prototypes. It is likewise much more secure to test in a wind tunnel than out in the open. The following explanation covers the concept of the wind tunnels and techniques for testing the NACA 0015 airfoil. A NACA 0015 airfoil, made of ABS materials and mounted in the center of the test section was used for this experiment as shown in Figure 34.

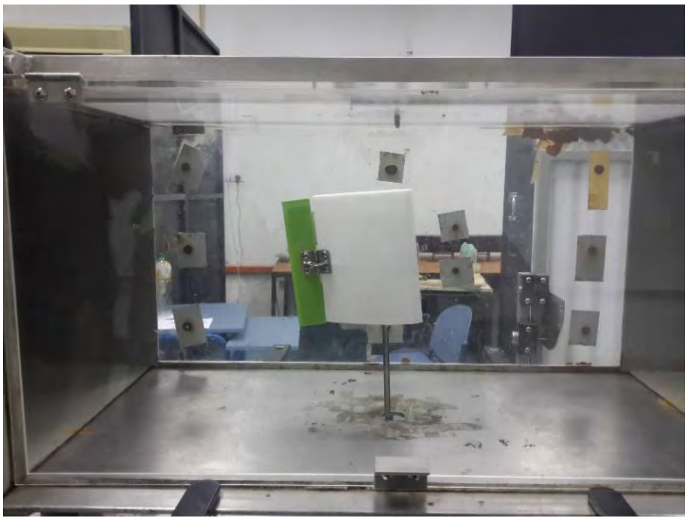

Figure 34 : Test section in a wind tunnel

During a test, the model is placed in the test section of the tunnel and air is made to flow past the model. Various types of instrumentation are used to determine the forces on the model. The airfoil has a 130mm in chord, extended the full width of the tunnel. A handle outside of the wind tunnel and attached to the airfoil was used to adjust the angle of attack. This was determined using a protractor. also mounted on the outside of the test section. In this case, there are two types of angle that is changes which are angle of attack and angle of flap. The airfoil was set at a 0 degree angle of attack and the wind tunnel operated at approximately 9.5 m/s. The air velocity in a wind tunnel is set manually be referring the wind velocity test section which include contraction section differential pressure vs velocity (Figure 35). The angle of attack is set at 0, 5, 10, 15 and 20 degrees and it was varied while taking note of the behaviour of the small streamers on the suction side of the airfoil. In addition, the value of angle of flap is set at 30 degrees. The points of separation and reattachment were noted. The angle of flap then was set at approximately 60 degrees and the wind tunnel velocity varied again taking note of the streamers as the flow separates and reattaches at the same speed. The same step then is repeated using angle of attack of 60 degrees.

Figure 35 : Wind velocity test section

Based on this experiment, the value of drag force and lift force are determined. Drag force can be defined as in fluid mechanics, the force which exerted on the solid object in the upstream direction of the relative flow velocity. Drag force depends on flow velocity and it decreases the fluid velocity. Therefore, drag force also called air resistance or fluid resistance. Contrasts with the drag force, lift force exerts when a fluid flowing pass through the surface of an object and the direction of lift is perpendicular to the flow velocity direction. Figure 36 show the relationship between drag and lift force.

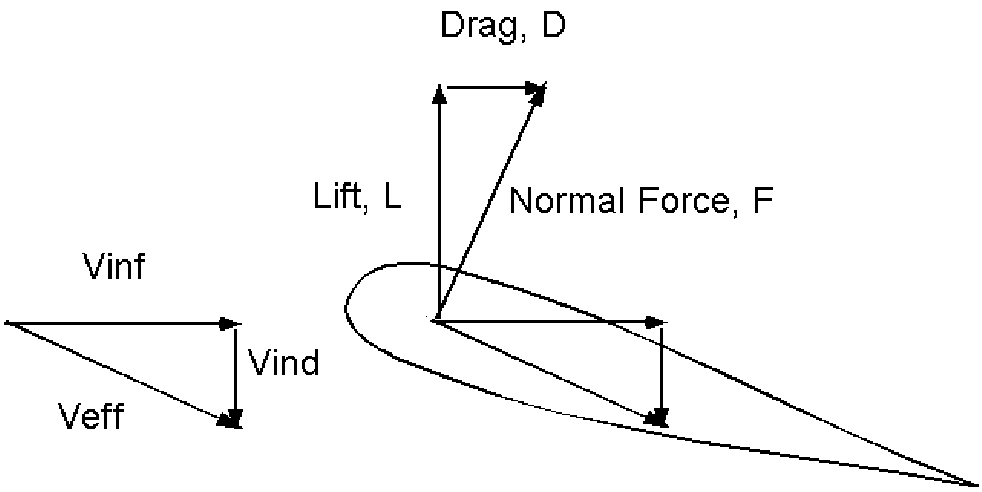

Figure 36 : Relationship between lift and drag

CHAPTER 4

RESULTS AND DISCUSSION

4.1 OVERVIEW

In order to increase the wind capture ability of the wind turbine, many research studies on the lift enhancement method of the wind turbine airfoil have been conducted by scholars at home and abroad. An airfoil with tailing edge flaps has a much higher lift-to-drag ratio than an airfoil without trailing edge flaps. Among all the lift enhancement methods of trailing edge flaps, the structure of the wind turbine airfoil with discrete trailing edge flaps is simple, the cost of production is low, and it can easily achieve variable angle control. But the aerodynamic performance of the wind turbine airfoil with traditional discrete trailing edge flaps has not been comprehensively studied, and gaps between the flaps and the airfoil main body has an influence on the aerodynamic performance of the airfoil. So, it is necessary to optimize the gap structure and study the aerodynamic performance of the discrete trailing edge flaps with different deflections angles.

In this study, the data and results of the drag force, lift force, drag coefficient and lift coefficient will be shown. Based on the experiment, the value of air velocity is constant which is 9.5m/s and the value of drag and lift force are collected during the experiment. Besides, this part will shows whether the experimental result can achieve the objective or not. The data and result obtained from the experiment are compared with the base case.

4.2 EXPERIMENTAL RESULTS AND ANALYSIS

4.2.1 Wind tunnel process

This wind tunnel is an open circuit downstream fan type, designed for subsonic aerodynamic studies in the experimental laboratory. Typical test capabilities are pressure and velocity measurement, estimation of drag and lift coefficients of an airfoil, pressure distribution around airfoil and cylinder, effect of instability of a “flutter wing”, and other basic aerodynamic tests.

The air enters the tunnel via a flare with flow straightener, wire mesh, contraction section. The test section is transparent. Downstream of the working section is a low angle diffuser which terminates at the tunnel fan. The diffuser and contraction sections have a high quality internal finish. The 7 blade fan impeller is an airfoil design cast aluminium to ensure maximum aerodynamic efficiency and minimum turbulence. Fan speed is adjustable by an inverter.

Four equally spaced static pressure taps are connected to a manifold at contraction section to minimize effects from a model and air speed is indicated by an inclined manometer. A graph of manometer reading us air speed is provided. Models are mounted on two components load cell support with indicators for measurement of drag and lift. Model holder can be rotated to allow quick change on the angle of incidence. This angle is indicated on an angular scale at the base of the holder. The tunnel is mounted on a self-contained bench with castors.

Table 1 : Technical data

PARTS	**SPECIFICATION**
Fan	480mm diameter
Motor	3.7kW 220V/380V, 3Ph, 50Hz
Inverter	5KVA
Contraction area ratio	7 : 1
Test section	300mm x 300mm x 450mm long
Maximum air velocity	Over 30m/s
Power supply	220V, 1Ph, 50Hz

4.2.2 Principle of lift and drag

Figure 37 shows the force acting on a body completely immersed in a relatively large expanse of flowing fluid. Let the free air stream or V be the uniform, undisturbed velocity some distance ahead of the body at rest. The fluid exerts a resultant force on the body, it is common practice to resolve this resultant force into two components. One component along the line of V is called the resistance or drag. The other component, at right angle to V, is called lift.

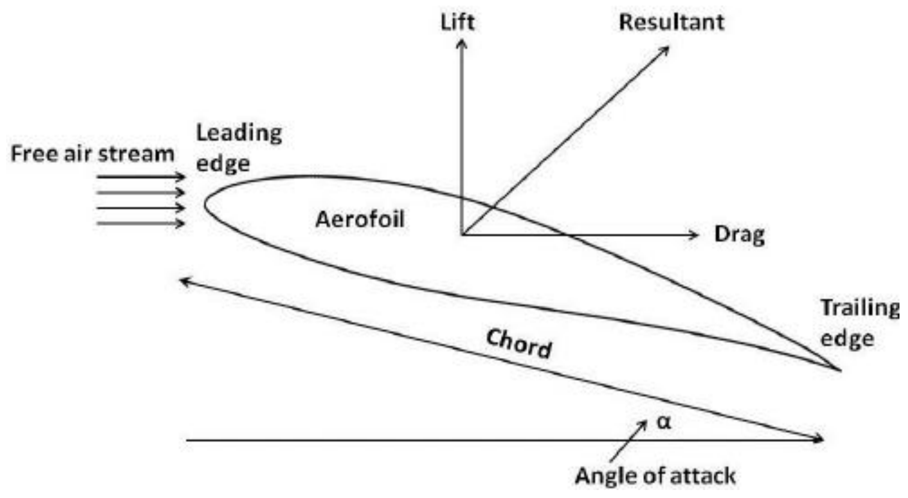

Figure 37 : Drag and lift force

The force exerted by a fluid on a body depends only on the relative velocity between body and fluid, and not on the absolute velocity of either fluid or body. The Figure 37 indicates one way of obtaining a certain relative motion. The same relative motion could be realized if the body were moving with the constant velocity V through a mass of fluid at rest some distance away from the body.

In general, lift and drag are usually considered in term of variable dimensionless index so-called “Lift Coefficient, C_L , and “Drag Coefficient, C_D” which can be expressed as follows:

$$C_L = \frac{L}{\frac{1}{2}\rho V^2 A} \tag{1}$$

$$C_D = \frac{D}{\frac{1}{2}\rho V^2 A} \tag{2}$$

Where:

A = Characteristic area of the object which is normally a projected area drawn around the peripheral profile of the object to the end at the plane.

V = Upstream wind velocity.

ρ = Density of air.

4.2.3 NACA 0015 airfoil with zero flap deflection

In this study, experimental and numerical analyses were performed. The experiments were conducted at 9.5 m/s wind velocity (V). Lift and drag coefficient of NACA 0015 airfoil at different attack angle between 0° and 20° were measurement. Airfoils have various shape and sizes. Therefore, non–dimensional coefficients (lift and drag coefficients) were taken into consideration to evaluate the advantages and disadvantages of airfoils. The lift and drag coefficient at wind tunnel test for NACA 0015 airfoil were measured as experimentally. Figure 38 shows the experimental setup for the base case.

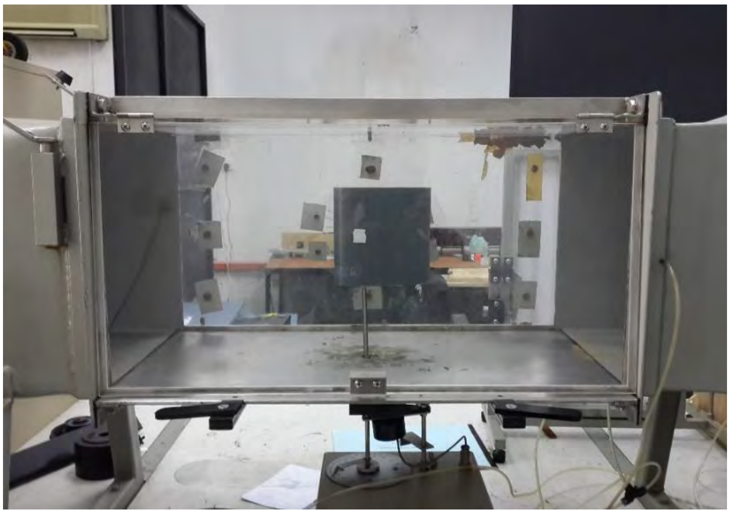

Figure 38 : Experimental setup for the base case

4.2.3.1 Sample calculation for airfoil NACA 0015 at 5 degree angle of attack

Principle dimensions :

Distance X = 89 mm

Cross-section area, Chord = 130 mm

Width = 130 mm

A = 130 x 130 = 16900 mm^2

= 0.0169 m^2

Indicated Drag Force (D_o) = 0.02 N, Standard distance (X_S) = 320 mm

Actual Drag Force (D) = D N, Actual distance (X_A) = 409 mm

DX_A = D_oX_S

D x 409 = 0.02 x 320

D = 0.016 N

Indicated Lift Force (L_o) = 0.1 N, Standard distance (X_S) = 250 mm

Actual Lift Force (L) = L N, Actual distance (X_A) = 339 mm

$$LX_A = L_oX_S$$

$$L \times 339 = 0.1 \times 250$$

$$L = 0.07 \text{ N}$$

Wind Tunnel Actual Measurement

Drag Force D = 0.016 N   Lift Force L = 0.07 N

Wind Velocity = 9.5 m/s   Air Temperature, T = 35 °C

From air property table at the measured room temperature, the following air properties is obtained :

At 35 °C, Air density ρ = 1.146 kg/m^3

Therefore, from Equation 1 and Equation 2, this calculation is obtained :

$$\text{Drag Coefficient, } C_D = \frac{0.016\ kg\,\frac{m}{s^2}}{\frac{1}{2}\,(1.146)\,\frac{kg}{m^3}\,(9.5^2)\,\frac{m^2}{s^2}\,(0.0169)\ m^2}$$

$$= 0.018$$

Note : N = $kg\ \frac{m}{s^2}$

Lift Coefficient, $C_L = \dfrac{0.07\ kg\ \frac{m}{s^2}}{\frac{1}{2}(1.146)\ \frac{kg}{m^3}\ (9.5^2)\ \frac{m^2}{s^2}\ (0.0169)\ m^2}$

= 0.08

Result for this experiment is shown in Table 2.

Table 2 : Result for base case

ANGLE OF ATTACK (DEGREE)	**INITIAL FORCE (N)**		**FINAL FORCE (N)**		**INDICATED FORCE (N)**		**ACTUAL FORCE (N)**		**COEFFICIENT**		**LIFT/ DRAG RATIO**
α (°)	**LIFT**	**DRAG**	**LIFT**	**DRAG**	**LIFT**	**DRAG**	**LIFT**	**DRAG**	C_L	C_D	C_L/C_D
0	-0.10	-0.29	-0.10	-0.29	0	0	0	0	0	0	0
5	-0.10	-0.29	-0.20	-0.31	0.1	0.02	0.07	0.016	0.080	0.018	4.444
10	-0.10	-0.30	-0.30	-0.41	0.2	0.11	0.15	0.086	0.172	0.098	1.755
15	-0.10	-0.30	-0.50	-0.35	0.4	0.05	0.29	0.039	0.332	0.045	7.378
20	-0.10	-0.29	-0.70	-0.33	0.6	0.04	0.44	0.031	0.503	0.035	14.371

4.2.3.2 Graph analysis

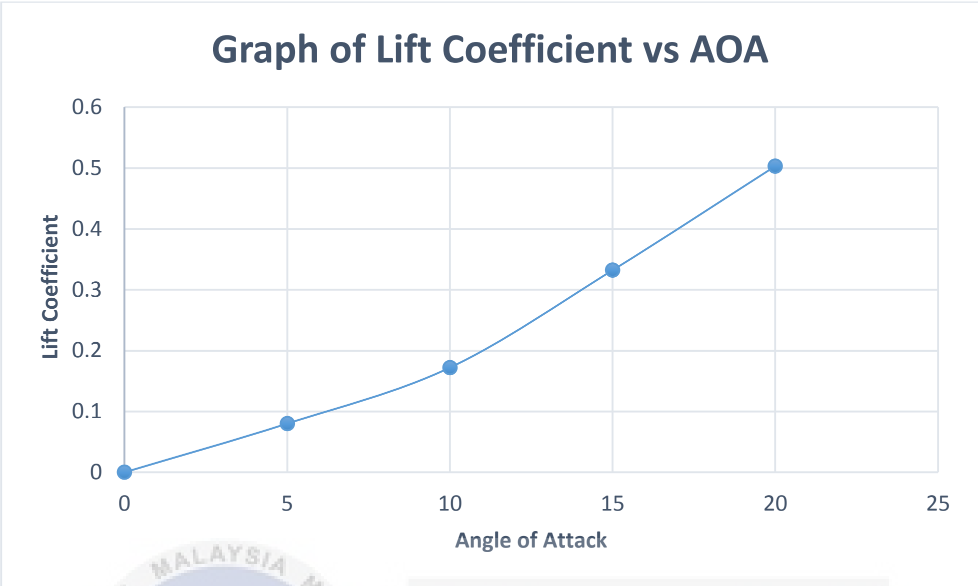

Figure 39 : Lift coefficient vs angle of attack for zero degrees of flap

The lift and drag coefficient at wind tunnel test for NACA 0015 airfoil were measured as experimentally. The maximum lift coefficient was found as 0.503 for 20° attack angle. The lift coefficient was primarily effected by attack angle as regards both increasing and decreasing. If attack angle increased, lift and drag coefficient could increase until a certain angle. Based on this graph, the lift coefficient is increasing from 0 to 0.503. Besides, a symmetrical wing has zero lift coefficient at 0 degrees angle of attack.

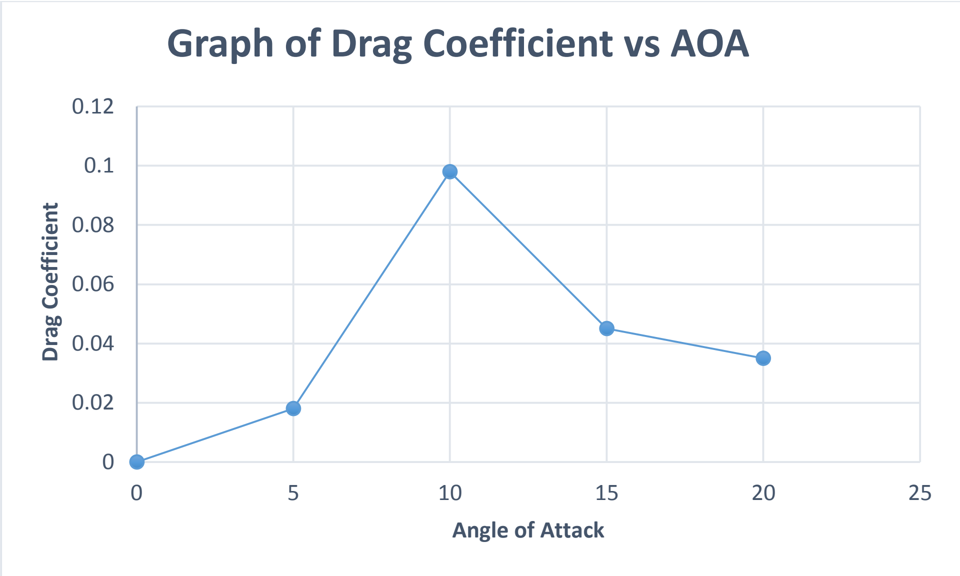

Figure 40 : Drag coefficient vs angle of attack for zero degrees of flap

The result showed that the value of a drag coefficient was increasing from 0 to 0.018, and kept increasing to 0.098 for 10°. The drag coefficient was primarily effected by attack angle as regards both increasing and decreasing. If attack angle increased, drag coefficient could increase until a certain angle. The drag coefficient is a number that aerodynamicists use to model all of the complex dependencies of shape, inclination, and flow conditions on aircraft drag.

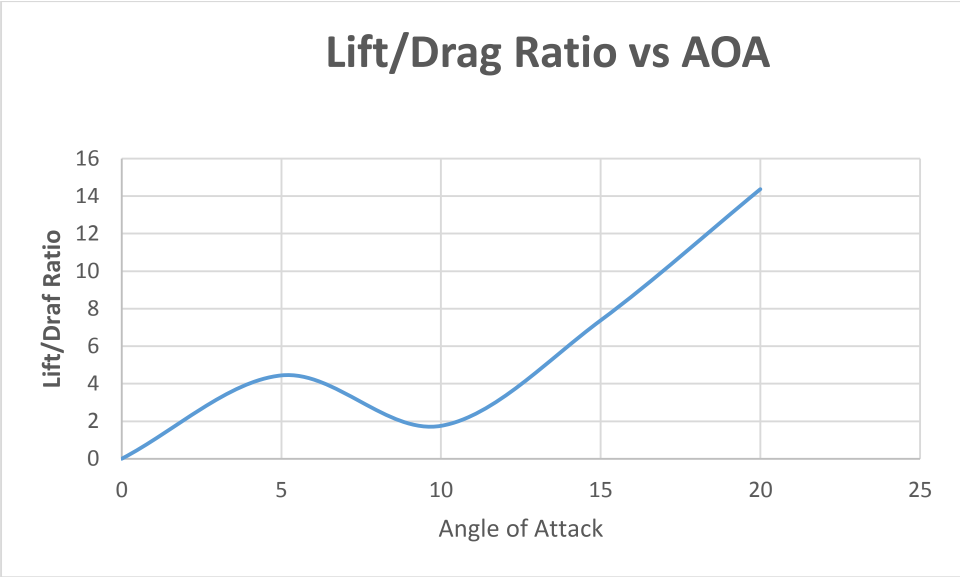

Figure 41 : Lift/Drag vs angle of attack for zero degrees of flap

The ratio of lift to drag is an indication of the aerodynamic efficiency of the airplane. Aerodynamicists call the lift to drag ratio the L/D ratio, pronounced "L over D ratio". An airfoil has a high L/D ratio if it produces a large amount of lift or a small amount of drag. So, based on the Figure 41, the highest value of lift/drag ratio is 14.371 at 20 degrees angle of attack. The lowest value is 0 at zero degrees angle of attack.

4.2.4 NACA 0015 at 10 degree angle of attack with 30 degree angle of flap.

Taking a wind turbine airfoil S809 as the research object, the structure of the discrete trailing edge flaps was designed, the chord length was set as 130 mm, and there is no gap between the flap and the main body of airfoil. Then the trailing edge flaps model was established. The flap rotates around the rotate center to form a different flap model at different deflect angles, the deflect angles of the flap varied from 0 - 20°. The experimental setup for this part is shown in Figure 41 which belongs to the airfoil with angle of flap at 30° and 60°.

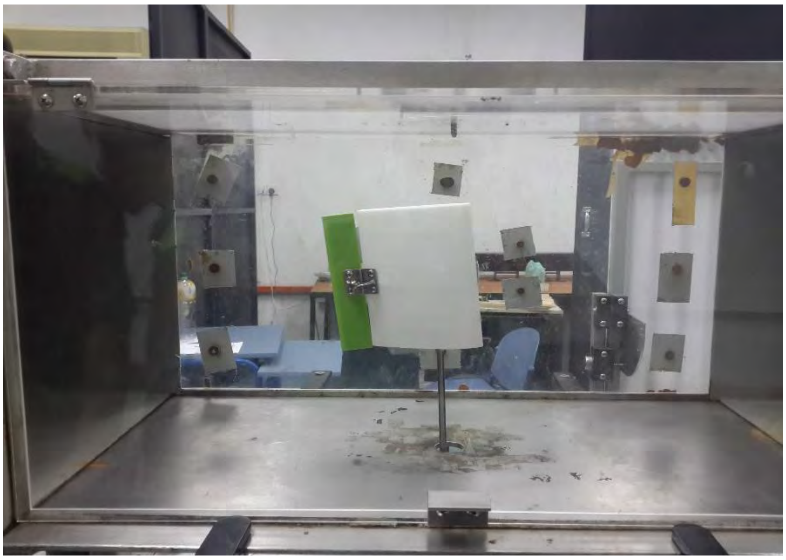

Figure 42 : Experimental setup for airfoil with flap

4.2.4.1 Sample calculation for airfoil NACA 0015 at 10 degree angle of attack with 30 degree angle of flap.

Principle dimensions :

Distance X = 89 mm

Cross-section area, Chord = 130 mm

Width = 130 mm

A = 130 x 130 = 16900 mm^2

= 0.0169 m^2

Indicated Drag Force (D_o) = 0.02 N, Standard distance (X_S) = 320 mm

Actual Drag Force (D) = D N, Actual distance (X_A) = 409 mm

DX_A = $D_o X_S$

D x 409 = 0.05 x 320 D = 0.039 N

Indicated Lift Force (L_o) = 0.1 N, Standard distance (X_S) = 250 mm

Actual Lift Force (L) = L N, Actual distance (X_A) = 339 mm

LX_A = $L_o X_S$

L x 339 = 0.5 x 250

L = 0.37 N

Wind Tunnel Actual Measurement

Drag Force D = 0.039 N Lift Force L = 0.37 N

Wind Velocity = 9.5 m/s Air Temperature, T = 35 °C

From air property table at the measured room temperature, the following air properties can be obtained :

At 35 °C, Air density ρ = 1.146 kg/m^3

Therefore, from Equation 1 and Equation 2, this calculation is obtained :

$$\text{Drag Coefficient, } C_D = \frac{0.039\ kg\,\frac{m}{s^2}}{\frac{1}{2}\,(1.146)\,\frac{kg}{m^3}\,(9.5^2)\,\frac{m^2}{s^2}\,(0.0169)\ m^2}$$

= 0.045

Note : N = $kg\ \frac{m}{s^2}$

Lift Coefficient, $C_L = \dfrac{0.37\ kg\,\frac{m}{s^2}}{\frac{1}{2}(1.146)\,\frac{kg}{m^3}\,(9.5^2)\,\frac{m^2}{s^2}\,(0.0169)\ m^2}$

$= 0.423$

Result for this experiment is shown in Table 3.

Table 3 : Result for slap at 30 degrees

ANGLE OF ATTACK (DEGREE)	INITIAL FORCE (N)		FINAL FORCE (N)		INDICATED FORCE (N)		ACTUAL FORCE (N)		COEFFICIENT		LIFT/ DRAG RATIO
α (°)	LIFT	DRAG	LIFT	DRAG	LIFT	DRAG	LIFT	DRAG	C_L	C_D	C_L/ C_D
0	-0.10	-0.24	0.17	-0.22	0.27	0.02	0.20	0.016	0.229	0.018	12.722
5	-0.10	-0.25	0.34	-0.20	0.44	0.05	0.32	0.039	0.366	0.045	8.133
10	-0.10	-0.22	0.40	-0.27	0.50	0.05	0.37	0.039	0.423	0.045	9.400
15	-0.10	-0.23	0.54	-0.31	0.64	0.08	0.47	0.063	0.538	0.072	7.472
20	-0.10	-0.23	0.68	-0.25	0.78	0.02	0.58	0.016	0.664	0.018	36.888

4.2.4.1.1 Graph analysis

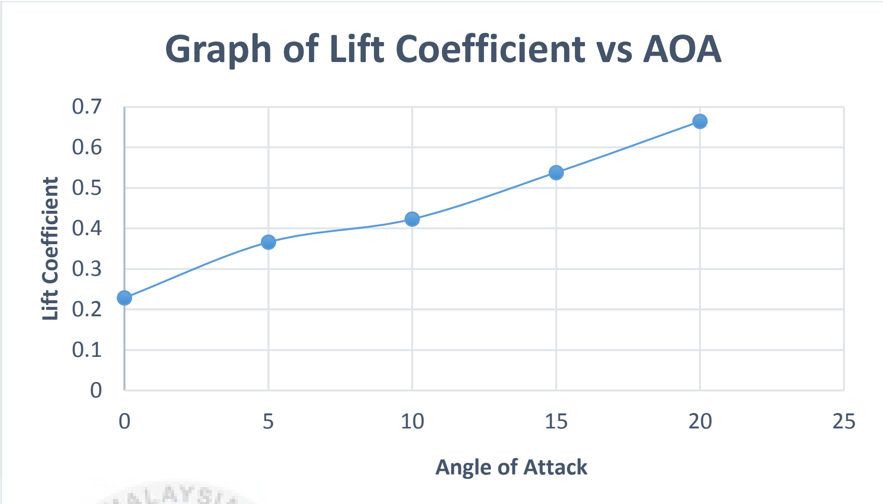

Figure 43 : Lift coefficient vs angle of attack for 30 degrees of flap

Looking at the measured lift coefficient it is apparent that the airfoil was not suffered from a severe loss of lift somewhere between the angles of 0.229 and 0.664 degrees. So there is no point at which the flow separated from the suction side of the airfoil causing the stalled condition. Theoretical values for the lift coefficient match closely to those measured but begin to deviate after the 20 degree point. This is a breakdown in the thin airfoil theory as the airfoil approaches the stall conditions.

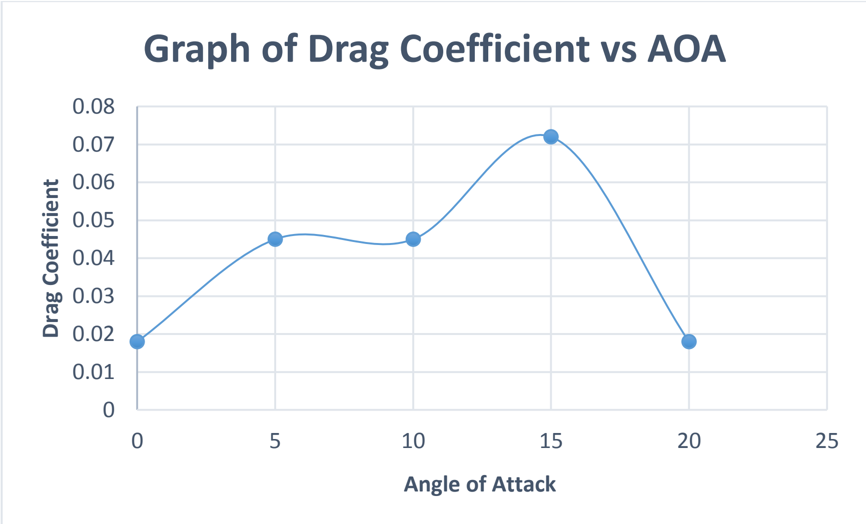

Figure 44 : Drag coefficient vs angle of attack for 30 degrees of flap

C_D has its minimum value at small angles of attack which is 0 degrees. As the stall angle is approached, the drag increases at a progressively higher rate due to separated flow. The minimum drag occurs at a fairly low angle of attack, in this case slightly at 0 degree angle of attack. At each angle of attack, the lift/drag ratio is the ratio between lift and drag or between the coefficient of lift and the coefficient of drag. Drag coefficient was constant from 5 to 10 degrees angle of attack and increase from 10 degrees angle of attack to 15 degrees angle of attack. The minimum value of drag coefficient is 0.018 while the highest value is 0.072.

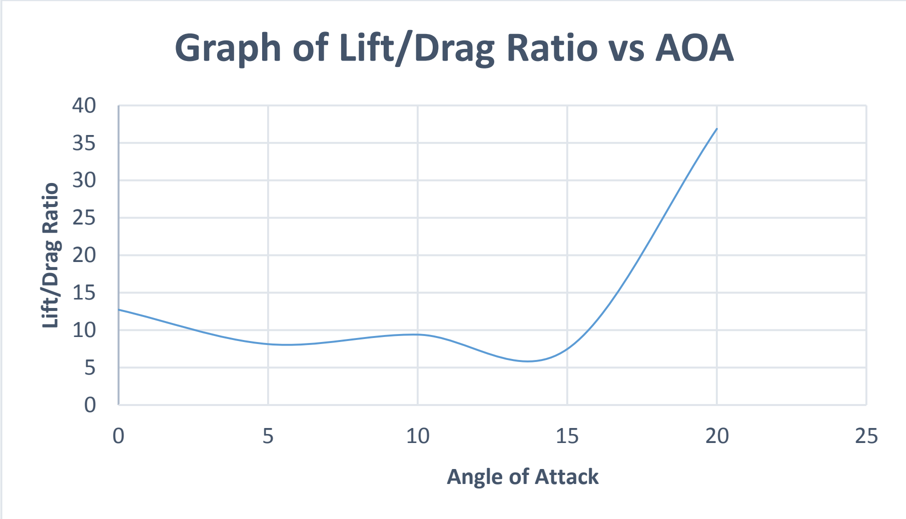

Figure 45 : Lift/Drag Ratio for 30 degrees of flap

For a light aircraft with a normally cambered wing, when the angle of attack is increased, the L/D ratio rapidly increases from zero to the maximum value. Then, as the angle of attack is increased further, the L/D ratio decreases until the stalling angle is reached and keeps decreasing even beyond that angle as shown in Figure 45 the stalling angle is between 0 and 5 degrees angle of attack, and between 10 and 15 degrees of attack. The reason for this behaviour is that when the angle of attack is increased until the lift/drag ratio reaches its maximum value, both C_L and C_D increase but C_L increases more than C_D.

4.2.4.2 Sample calculation for airfoil NACA 0015 at 15 degree angle of attack with 60 degree angle of flap.

Distance X = 89 mm

Cross-section area, Chord = 130 mm

Width = 130 mm

A = 130 x 130 = 16900 mm^2

= 0.0169 m^2

Indicated Drag Force (D_o) = 0.02 N, Standard distance (X_S) = 320 mm

Actual Drag Force (D) = D N, Actual distance (X_A) = 409 mm

$$DX_A = D_o X_S$$

$$D \times 409 = 0.04 \times 320$$

$$D = 0.031 \text{ N}$$

Indicated Lift Force (L_o) = 0.1 N, Standard distance (X_S) = 250 mm

Actual Lift Force (L) = L N, Actual distance (X_A) = 339 mm

$$LX_A = L_o X_S$$

$$L \times 339 = 0.98 \times 250$$

$$L = 0.72 \text{ N}$$

Wind Tunnel Actual Measurement

Drag Force D = 0.031 N Lift Force L = 0.72 N

Wind Velocity = 9.5 m/s Air Temperature, T = 35 °C

From air property table at the measured room temperature, the following air properties can be obtained :

At 35 °C, Air density ρ = 1.146 kg/m^3

Therefore, from Equation 1 and Equation 2, this calculation is obtained:

$$\text{Drag Coefficient, } C_D = \frac{0.031\ kg\,\frac{m}{s^2}}{\frac{1}{2}(1.146)\,\frac{kg}{m^3}\,(9.5^2)\,\frac{m^2}{s^2}\,(0.0169)\ m^2}$$

$$= 0.035$$

Note : N = $kg\ \frac{m}{s^2}$

$$\text{Lift Coefficient, } C_L = \frac{0.72\ kg\,\frac{m}{s^2}}{\frac{1}{2}(1.146)\,\frac{kg}{m^3}\,(9.5^2)\,\frac{m^2}{s^2}\,(0.0169)\ m^2}$$

$$= 0.824$$

Result for this experiment is shown in Table 4.

Table 4 : Result for slap at 60 degrees

ANGLE OF ATTACK (DEGREE)	INITIAL FORCE (N)		FINAL FORCE (N)		INDICATED FORCE (N)		ACTUAL FORCE (N)		COEFFICIENT		LIFT/ DRAG RATIO
α (°)	LIFT	DRAG	LIFT	DRAG	LIFT	DRAG	LIFT	DRAG	C_L	C_D	C_L/C_D
0	-0.10	-0.27	0.23	-0.28	0.33	0.01	0.24	0.008	0.275	0.009	30.555
5	-0.10	-0.26	0.45	-0.29	0.55	0.03	0.41	0.023	0.469	0.026	18.038
10	-0.10	-0.26	0.74	-0.31	0.84	0.05	0.62	0.039	0.709	0.045	15.755
15	-0.10	-0.25	0.88	-0.29	0.98	0.04	0.72	0.031	0.824	0.035	23.543
20	-0.10	-0.26	0.70	-0.27	0.80	0.01	0.59	0.008	0.675	0.009	75.000

4.2.4.2.1 Graph analysis

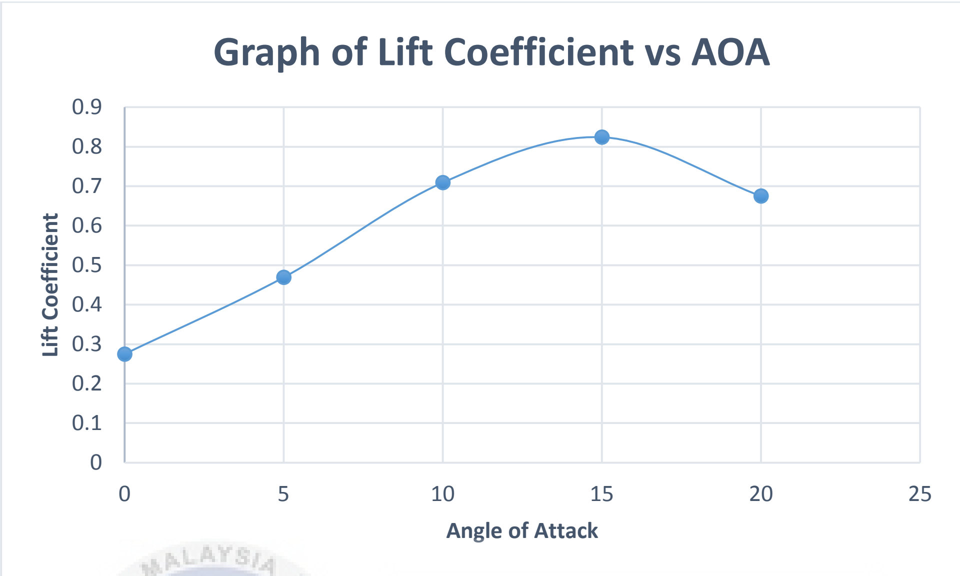

Figure 46 : Lift coefficient vs angle of attack for 60 degrees of attack

The lift coefficient of a fixed-wing aircraft varies with angle of attack. Increasing angle of attack is associated with increasing lift coefficient up to the maximum lift coefficient, after which lift coefficient decreases. As the angle of attack of a fixed-wing aircraft increases, separation of the airflow from the upper surface of the wing becomes more pronounced, leading to a reduction in the rate of increase of the lift coefficient. The critical angle of attack is the angle of attack which produces maximum lift coefficient. This is also called the "stall angle of attack". Based on this graph, the stall angle of attack is at 15 degrees which has the highest value of lift coefficient, 0.824.

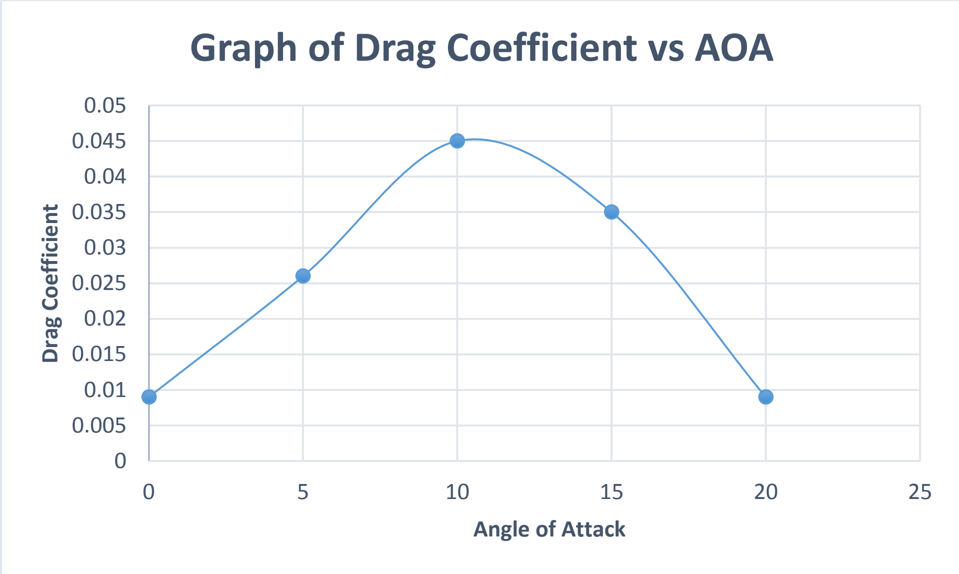

Figure 47 : Drag coefficient vs angle of attack for 60 degrees of flap

The plot at the right of the figure shows how the drag varies with angle of attack for a typical thin airfoil. At low angles, the drag is nearly constant. Notice on this plot that at zero angle, a small amount of drag is generated because of skin friction and the airfoil shape. At the right of the curve, the drag changes rather abruptly and the curve stops. However, once the wing stalls, the flow becomes highly unsteady and the value of the drag changes rapidly with time because it is so hard to measure such flow conditions. We can see that the lowest value of drag coefficient is 0.009 at 20 degrees angle of attack. This means the value of drag coefficient shows the best result among 3 cases.

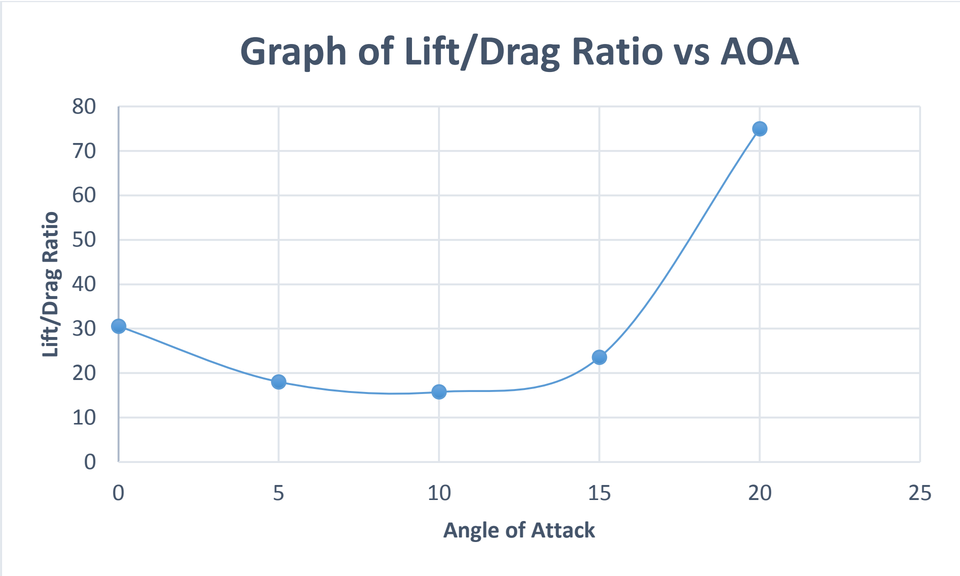

Figure 48 : Lift/Drag ratio vs angle of attack for 60 degrees of flap

The smaller the angle between C_L axis and the straight line, the greater the lift/drag ratio. Based Figure 48, the best value of lift/drag ratio is 75.000 at 20 degrees angle of attack depending on several factors concerning the wings. The angle of attack at which we obtain the best lift/drag ratio is called the Most Efficient Angle of Attack. As the amount of lift varies with the angle of attack, so too does the drag. Thus, although it is desirable to obtain as much lift as possible from a wing, this cannot be done without increasing the drag. It is therefore necessary to find the best compromise.

4.3 LIFT AND DRAG ANALYSIS

The lift coefficient of an airfoil varies with angle of attack. Increasing angle of attack is associated with increasing lift coefficient up to the maximum lift coefficient, after which lift coefficient decreases. As the angle of attack of an airfoil increases, separation of the airflow from the upper surface of the wing becomes more pronounced, leading to a reduction in the rate of increase of the lift coefficient. A symmetrical wing has zero lift at 0 degrees angle of attack. The lift curve is also influenced by the wing shape, including its airfoil section. Therefore, the higher value of the lift coefficient produces a better result.

All items that affect the aeroplane's drag, affect C_L/ C_D ratio as well. Increasing drag at a given C_L increases the C_L/ C_D ratio, thus decreases C_L/ C_D ratio. These items are:

- Wing section. The wing section with the lowest drag yields the best C_L/ C_D ratio.
- Use of flaps. Deployment of high lift devices will in most cases increase the drag. Only when being near or at speeds for stall for a clean wing can the use of flaps reduce drag somewhat but during all other flight conditions, high lift devices reduce the lift/drag ratio.
- Aspect ratio. Because a high aspect ratio reduces the induced drag, the C_L/ C_D ratio at a certain C_L is high when the aspect ratio is high.
- Aeroplane mass. At the same speed, the C_L/ C_D ratio is higher when the mass is higher. However, at a higher speed, when the C_L value is equal to the C_L at the lower mass, the C_L/ C_Dratios are also equal.
- Wing planform. The wing planform with the lowest induced drag yields the best C_L/ C_D ratio.
- Aeroplane speed (AOA). The speed with the minimum drag yields the best C_L/ C_D ratio.

CHAPTER 5

CONCLUSION AND RECOMMENDATION

5.1 CONCLUSION

The NACA 0015 airfoil was analysed for the lift, drag and moment coefficients as planned. The measured values determined from lab data agree correctly with the theoretical values for the lift, drag and quarter chord moment. A stabilizing or restoring moment was observed after the stall occurred. The drag and lift coefficient were clearly observed with respect to the free air velocity and angle of attack. This was accomplished by the condition of the airfoil in the test section. For the base case, the highest value of the lift coefficient is 0.503 and the lowest value of drag coefficient is 0.018. For the second case which is an airfoil with 30 degrees angle of flap, it shows better result because the highest value of lift coefficient is 0.664. For 60 degrees angle of flap, the highest value of lift coefficient is 0.824 and the lowest value of drag coefficient is 0.009. This result can conclude that an airfoil have a better result with an addition of angle of flap. In addition, throughout the previous research and theoretically, an airplane need a higher value of lift coefficient because once the aircraft is on the ground, the flaps may decrease the effectiveness of the brakes since the wing is still generating lift and preventing the entire weight of the aircraft from resting on the tires, thus increasing stopping distance, particularly in wet or ice conditions.

The deflect angle of the discrete trailing edge flaps had much influence on the aerodynamic performance of the model. With the increase of the deflect angle, the camber of airfoil was increased, this made the airflow near trailing edge of airfoil deflected downward, the velocity of airflow near the upper surface of airfoil increased, eventually leading to enhancement of the lift coefficient and the lift-to-drag ratio of the airfoil with discrete trailing edge flaps. The drag of the airfoil decreased with the increase of attack angle at first and then increased with the increase of attack angle. Depending on the aircraft type, flaps may be partially extended for takeoff. When used during takeoff, flaps trade runway distance for climb rate: using flaps reduces ground roll but also reduces the climb rate. The amount of flap used on takeoff is specific to each type of aircraft, and the manufacturer will suggest limits and may indicate the reduction in climb rate to be expected.

The critical angle of attack is the angle of attack which produces maximum lift coefficient. This is also called the "stall angle of attack". Below the critical angle of attack, as the angle of attack increases, the coefficient of lift (C_L) increases. Conversely, above the critical angle of attack, as angle of attack increases, the air begins to flow less smoothly over the upper surface of the airfoil and begins to separate from the upper surface. On most airfoil shapes, as the angle of attack increases, the upper surface separation point of the flow moves from the trailing edge towards the leading edge. At the critical angle of attack, upper surface flow is more separated and the airfoil or wing is producing its maximum coefficient of lift. As angle of attack increases further, the upper surface flow becomes more and more fully separated and the airfoil produces less coefficient of lift.

5.2 RECOMMENDATION

There are two recommendations that related to this study. First, the value of angle of attack need to be higher than 20 degree to get a better result. This is because when angle of attack is low, there is no "angle of stall" during the wind tunnel test and based on a graph of lift coefficient vs angle of attack. Second, the value of air velocity that are flowing into the test section must be higher to achieve the best result. Since the wind tunnel in a mechanical engineering laboratory have a problem on adjusting the velocity, so we can't get the best result by try and error setting up the value of free air velocity. Besides, the condition of the airfoil that has to be examined must in a good condition to prevent an error and wrong results.

REFERENCES

Jared Carr, Rafael Ferraz, Songqi Gao, Aaron Jameson, Chang Yul Lee, Daniel Lu, Aaron Wienkers, Cheng Hao Yuan, 2014, Investigation of the Effect of Tubercles on Airfoil Performance.

Steven D. Miller, 2008, LIFT, DRAG AND MOMENT OF A NACA 0015 AIRFOIL.

Li Nan, 2013, The methods of drag force measurement in wind tunnels, by FACULTY OF ENGINEERING AND SUSTAINABLE DEVELOPMENT.

Inclination Effects on Drag, Retrieved from https://www.grc.nasa.gov/www/k-12/airplane/inclind.html.

Dr. J. M. Meyers, Dr. D. G. Fletcher, Dr. Y. Dubief, Lift and Drag on an Airfoil, ME 123: Mechanical Engineering Laboratory II: Fluids.

Nongye Gongcheng Xuebao, 2014, Aerodynamic performance of discrete trailing edge flaps of wind turbine airfoil

Lift Force and Drag Force, Retrieved from http://www.symscape.com/lift-force-and-drag-force

NUMERICAL AND EXPERIMENTAL INVESTIGATIONS OF LIFT AND DRAG PERFORMANCES OF NACA 0015 WINF TURBINE AIRFOIL BY ADEM ACIR et al. (2015)

RANS SIMULATIONS OF AERODYNAMIC PERFORMANCE OF NACA 0015 FLAPPED AIRFOIL BY SOHAIB OBEID et al. (2016)

INFLUENCE OF INFLOW ANGLE ON FLEXIBLE FLAP AERODYNAMIC PERFORMANCE BY H Y ZHAO et al. (2007)

INVESTIGATION OF THE EFFECT OF TUBERCLES ON AIRFOIL PERFORMANCE BY JARED CARR et al. (2014)